Mutual Information Analysis of Lower Leg Muscle sEMG Signals to Examine Neural Connectivity and Postural Control During Various Quiet Standing Tasks: A Pilot Study

Gordon Alderink *, Diana McCrumb, David W. Zeitler, Samhita Rhodes

Posted Date: 2 April 2026

doi: 10.20944/preprints202604.0137.v1

Keywords: postural control; inverted pendulum model; ankle strategy; common neural drive; magnitude square coherence; entropy; mutual information

 doi:10.20944/preprints202604.0137.v1

Article

Mutual Information Analysis of Lower Leg Muscle sEMG Signals to Examine Neural Connectivity and Postural Control During Various Quiet Standing Tasks: A Pilot Study

Gordon Alderink [1,*], Diana McCrumb [2], David W. Zeitler [3] and Samhita Rhodes [4]

[1] Department of Physical Therapy & Athletic Training, Grand Valley State University, Grand Rapids, MI 49503

[2] BAMF Health, Grand Rapids, MI 49503

[3] Department of Statistics, Grand Valley State University, Allendale, MI 49401

[4] School of Engineering, Grand Valley State University, Grand Rapids, MI 49504

* Correspondence: aldering@gvsu.edu

Abstract

In bipedal stance the central nervous system implements a pre-programmed ankle strategy to maintain upright balance and respond to internal perturbations. This strategy comprises a synchronized common neural drive delivered to synergistically grouped muscles. This study evaluated the normalized mutual information (MI) between surface electromyographic (EMG) signals of unilateral and bilateral homologous muscle pairs of the lower legs during various quiet standing tasks in normal healthy adults. The leg muscles examined included the right and left tibialis anterior (TA), medial gastrocnemius (MG), and soleus (S). MI, an information-theoretic measure that quantifies the reduction in uncertainty in predicting a signal from another known signal,, was estimated using MATLAB toolbox Mutual Information Distance and Entropy Reduction (MIDER). This method for inferring network structures from shared information between two signals was applied to pairs of filtered EMG signals in the alpha (8 – 13 Hz), beta (13 – 30 Hz), and gamma (30 – 100 Hz) neural frequency bands for feet together and feet tandem stances, under eyes open and eyes closed conditions. Results showed that normalized MI was greater in the medial gastrocnemius and soleus muscle pairs across the beta, lower gamma, and upper gamma frequency bands in the tandem standing posture under both eyes open and eyes closed conditions, and generally increased in antagonistic muscle pairs in less stable standing positions. It appears that functional muscle synergies are more important than limb dominance in tandem standing. Significant inter-trial and inter-participant variability is consistent with biological differences and control of a complex system. Our results suggest that the use of MI analyses in the clinical testing of tandem standing tasks might be a useful adjunct for persons with standing balance impairments.

Keywords: postural control; inverted pendulum model; ankle strategy; common neural drive; magnitude square coherence; entropy; mutual information

1. Introduction

Bipedal stance in humans is characterized by a variable and relatively narrow base of support (BoS), a higher center of mass (CoM), and a propensity for biomechanical instability. Control of static and dynamic standing postures declines with age, leading to an increase in postural sway [1]. Additionally, individuals with neurological and musculoskeletal disorders demonstrate poor balance control [2–5] and may have greater fall risk [6–8]. To prevent falls and related morbidity, the

 doi:10.20944/preprints202604.0137.v1

biomechanics and neural control of bipedal stance in healthy young and elderly adults, and individuals with disease, e.g., neuropathology, needs to be examined further.

The central nervous system (CNS) integrates the interactions of visual, vestibular, and somatosensory information to coordinate the muscle actions associated with the control of static postures and dynamic movements [9]. To generate joint movement, individual muscles are activated by the recruitment of thousands of specialized motor units (MU) through motor pools, i.e., groups of muscles. Thus, to achieve specific movement goals through muscle actions a redundancy problem, i.e., multiple degrees of freedom (DoF), is created [10,11]. Recognizing this, Bernstein [10] suggested that hierarchical control mechanisms within the CNS implemented specific functional control structures to limit the DoF at four levels: muscle tone, muscle synergies, space, and actions [10,12]. In essence, then, groups of muscles, i.e., synergies, act together to complete a similar act or function; that is, muscle synergies as functional "structures" comprise the minimal number of muscles needed to generate a movement(s) to accomplish a behavioral goal.

Our interest primarily rests in the examination, and extended understanding, of postural control during bipedal stance. Controlling internal and external perturbations of quiet stance is a fundamental activity of daily living. The single inverted pendulum (SIP) model has been widely used to quantify control strategies during the maintenance of standing balance, that is, controlling the continuous oscillation of the center of pressure (CoP) around the center of mass (CoM) during quiet standing [13–18]. The results from our research that focused on the control of quiet tandem stance reported that despite the inter-trial and participant variability neural commands to the leg muscles implied a task-sharing role. It was notable that the soleus was primarily tasked to keep the body upright, whereas the back-and-forth activity of the tibialis anterior and peroneus longus controlled the CoM in the frontal plane [13]. Although this descriptive information has provided some insights into the mechanical control of quiet standing, it is limited by inattention to the complexity of the system than manages muscle synergies and linear methods of analysis.

Other computation methods have attempted to elucidate the role muscle synergies play in addressing the DoF problem relative to balance control. Krishnamoorthy et al. [19,20] defined muscle (or M) modes of several standing postural muscles using integrated EMG and principal component analysis (PCA). Torres-Oviedo and Ting [21] extended that work by identifying muscle synergies related to the intra- and inter-trial variation of human postural control using non-negative matric factorization (NNMF) and Boonstra et al. [22] decomposed EMG envelopes from 10 leg muscles using NNMF and PCA to estimate the number of muscle synergies during different standing postural activities. Others [23,24] used EMG as input to neuromechanical models to examine quiet standing postures and other movements.

The frequency ranges associated with neural drive oscillations have been shown to suggest signals of origin in the CNS [25], as shown in Table 1. The strength of neural synchronization from these frequency bands can be identified through connectivity analyses, such as EMG-EMG coherence (magnitude-squared coherence or MSC), corticomuscular coherence (CMC), and intermuscular coherence (IMC) [26–28]. These methods have been used to examine common neural input to muscle groups related to a variety of activities including heel rise tasks [29], squatting [30], ballet positions [31], sitting and standing tasks involving persons with Parkinson's disease [32], and quiet bipedal standing [33,34].

Table 1. Neural frequency bands and possible origins.

Wave	Frequency (Hz)	Origin	Task Manifestation
Delta	0.5 – 4	Unknown	Isometric contraction, slow movements
Theta	4 – 8	Unknown	Isometric contraction, slow movements
Alpha	8 – 13	Unknown	Isometric contraction, slow movements
Beta	13 – 30	Motor cortex	Submaximal voluntary contraction
Lower Gamma	30 – 60	Motor cortex	Voluntary contraction, slow movements
Upper Gamma	60 – 100	Brainstem	Eye movement (60 – 90 Hz), respiration

 doi:10.20944/preprints202604.0137.v1

We found that EMG-EMG coherence increased when test conditions increased the difficulty of the task, e.g., unipedal and tandem stance [35–39], with greater coherence typically noted in the delta frequency band regardless of the muscle pair [40–42]. Beta band coherence, assumed to reflect activity in the corticospinal tract [25,43], generally varied with the complexity of standing tasks [36–39], suggesting that cortical control may increase as standing postures become more challenging. Research using EMG-EMG coherence measures to gain insight into relationships between muscles that compose functional synergies that provide standing postural control has certainly been rewarding. However, magnitude-squared coherence methods mainly measure linear connectivity in time and frequency domains and cannot give the direction of information flow [44,45].

We know that within neuronal pathways, dynamic interactions among several subsystems are mediated to support physiological function. Since, when measured, the neural connectivity associated within the CNS' hierarchical system generates non-linear time series whose nature cannot be captured using linear measures such as MSC, more appropriate measures are needed [44,45]. Information theory provides the foundations for investigating the flow and examination of information to the functional systems just described.

As an aspect of probability theory, Shannon's information theory is a rigorous and accurate approach to reliably quantify neural code as a mathematical framework for quantifying information transmission in communication systems [46–49]. A summary of the general framework of Shannon's theory is provided in Appendix A.

Mutual information quantifies the information shared between two random variables, i.e., time series, that is, MI measures the average reduction in uncertainty about one variable that results from the learning the value of the other. MI can also be thought as the measure of mutual dependence between the random variables. Since traditional correlation measures, such as covariance, autocorrelation, and magnitude-squared coherence, may not fully capture underlying structures of physiological signals due to their nonlinear nature, MI's ability to analyze the coupling between different signals and identify complex dependencies and interactions makes it more suitable to examine the multifaceted behavior of biological systems, in general, and those behaviors related to postural control in particular. Let's briefly examine how MI has been utilized in prior research. Several studies used MI to characterize linear and nonlinear information flow to examine wrist/hand function and reaching tasks that involved healthy individuals [50–54], as well as elderly [52] and persons with disability [55]. Mutual information analyses have also been applied to investigate the synchronization of electroencephalographic (EEG) measures in patients with epilepsy [56], examination of the EMG of lower extremity muscles in persons with freezing gait related to Parkinson's disease [57], and neuroimaging, e.g., EEG and magnetoencephalography [58].

However, there is a paucity of research applying MI analyses of various metrics, e.g., CoP, neuromuscular activations, etc. that are typically used in research related to quiet and perturbed standing balance. Wang et al. [59], using various standing balance tasks and active swaying, tested shared dependence between the CoP in the antero-posterior (A/P) and medio-lateral (M/L) directions and compared typically developing (TD) children and age-matched children with autism spectrum disorders (ASD). Those with ASDA showed deficits in both postural orientation and equilibrium processes and reduced ability to decouple distinct ankle and hip strategies. A similar study comparing TD individuals (aged 6-19 years) and those with autism during normal standing, active standing circular swaying, and stepping tasks examined shared dependencies of the CoP A/P and M/L excursions [60]. They showed that individuals with ASD demonstrated increased CoP trajectory lengths during stance activities and reduced MI during circular sway, suggesting a reduced ability to effectively coordinate distinct lower extremity joint movements to maintain stability.

Boonstra et al. [61] used a signal processing framework for the description of how information was processed by muscle networks [62] and multivariate information decomposition of several lower and upper extremity muscles to examine their functional interactions under nine experimental conditions. These researchers combined concepts of entropy and conditional entropy to measure

 doi:10.20944/preprints202604.0137.v1

mutual information and noted significant changes in muscle networks across postural tasks localized to the muscles involved in performing those tasks.

O'Reilly et al. [63] provided an overview of their use of partial information decomposition to demonstrate nested networks of functionally diverse inter- and intramuscular interactions with distinct functional consequences on task performances related to object-lifting and balancing on a balance board, comparing outcomes between young and older adults. They found that motor variability among older adults appeared to have a functional underpinning characterized by concurrent increases and decreases in functional integration at inter- and intramuscular scales

Few investigators [59–61,63] have used MI in their analyses of quiet standing and only one [63] examined the sEMG of selected lower extremity muscles across multiple frequency bands in applying MI analyses of standing balance. It seems clear that additional research using mutual information to study quiet standing balance tasks is needed. In a previous study [39], we examined the magnitude-squared coherence of sEMG time series of several lower leg muscles across several frequency bands related to normal and tandem standing. The purpose of this study was to use the EMG data to describe how MI may provide additional insights about the interactions and coordination of lower leg muscles during quiet standing in a cohort of healthy young adults. We were interested in noting how the MI between muscle pairs may change with less stable standing positions (feet together vs. tandem stance), under eyes-open or closed conditions, and whether placing the dominant limb back or forward made any difference.

2. Materials and Methods

2.1. Participants

Six (2 males and 4 females) healthy young adults (age: 24.8 ± 3.3 years; height 171.0 ± 10.5 cm; body mass: 71.0 ± 13.5 kg) comprised a sample of convenience and were recruited from the local University community. They were included if they were between 18-40 years old, were unrestricted in activities of daily living, did not have a history of neurological or musculoskeletal disorders, and had not sustained bone/joint injuries in the previous six months. Individuals were excluded if they reported any recent musculoskeletal injuries and did not fall within the desired age range. Before data collection commenced, leg/foot dominance for each participant was determined based on the leg with which they preferred to kick a ball. A follow-up task of standing on one leg was implemented for participants who were unable to determine a preference from the previously asked questions. Three participants were right-leg and three left-leg dominant (Table 2). The Human Research Review Committee approved this study, Institutional Review Board, Office of Research Compliance and Integrity, at Grand Valley State University (18-246-H).

Table 2. Participant demographics.

P	Gender	Foot Dominance	Age	Height (cm)	BM (kg)
P01	F	Right	26	170.4	64.5
P02	F	Right	21	162.6	64.7
P03	M	Left	23	174.7	63.9
P04	M	Left	28	190	98.2
P05	F	Right	25	163	70.1
P06	F	Right	25	164	63.2

P = participant; BM = body mass.

2.2. Experimental Protocol

 doi:10.20944/preprints202604.0137.v1

Participants completed five 30-second trials of six different standing balancing conditions (Table 3) starting with eyes open, feet together (EOFT). The EOFT position was subsequently defined as the most stable standing position, and served as the baseline to compare to other balance conditions. A 30-second break was implemented between trials and a 2-minute break between each condition. Test conditions were completed in the order listed in Table 3 for all participants.. Balance tasks were performed barefoot, and arms were positioned with the shoulders flexed slightly and elbows fully flexed so that the index finger pointed towards the ipsilateral shoulders.

Table 3. Quiet standing test conditions.

Balance Condition	Description
EOFT	Eyes Open, Feet Together
ECFT	Eyes Closed, Feet Together
EOTanDF	EO, Feet Tandem, Dominant Foot Forward
ECTanDF	EC, Feet Tandem, Dominant Foot Forward
EOTanDB	EO, Feet Tandem, Dominant Foot Back
ECTanDB	EC, Feet Tandem, Dominant Foot Back

2.3. Data Acquisition

Surface electromyographic (EMG) signals (1200 Hz; Motion Lab Systems Inc., Baton Rouge, LA), motion trajectories (120 Hz), and ground reaction forces (1200 Hz; Advanced Mechanical Technology Inc., Watertown, MA) were synchronized using Vicon NEXUS motion capture software v2.8 (Oxford Metrics, Oxford, UK). Only EMG data were used for analysis in this study.

Myoelectrical activity was recorded from the left (L) and right (R) tibialis anterior (TA), medial gastrocnemius (MG), and soleus (S) muscles [64]. These muscles were chosen because of their prominent role in standing postural control [13,14,17]. Preparation and application of electrodes followed SENIAM recommendations [65] (see [39] for details). Accurate electrode placement was verified by performing manual muscle tests for each muscle. A reference, i.e., ground, electrode was secured to the patella on one of the lower extremities. Possible motion artifacts due to movement of EMG cables was minimized by securing the electrodes and wires with pre-wrap.

The MLS MA-411 pre-amplifiers were used to record the EMG signals.. The pre-amplifiers were interfaced with the MA300-XVI EMG patient unit acquisition system. The patient unit of the MA-411 implemented a 500 Hz low-pass anti-aliasing filter on the raw EMG before transmitting it to the desktop unit where the signal was further filtered with a 10 Hz high-pass filter. Raw EMG signals from a representative participant for each muscle were checked as described by [37]. All recorded EMG signals were analyzed in the frequency domain using MATLAB R2018a (The MathWorks, Natick, MA) for the following neural frequency bands (Table 4) and muscle pairs (Table 5) to observe the presence of synchronized correlated neural drives.

Table 4. Neural frequency bands of interest.

Bands	Range (Hz)
Delta	0 - 4
Theta	4 – 8
Apha	8 – 13
Beta	13 – 30
Lower Gamma	30 – 60
Upper Gamma	60 - 100

 doi:10.20944/preprints202604.0137.v1

Delta and theta frequency bands were omitted from final analyses because of their susceptibility to motion artifact.

Table 5. Muscle pairs analyzed.

Left Unilateral	Right Unilateral	Bilateral Homologous
LTA:LMG	RTA:RMG	LTA:RTA
LTA:LS	RTA:RS	LMG:RMG
LMG:LS	RMG:RS	LS:RS

LTA:RTA = left and right tibialis anterior; LMG:RMG = left and right medial gastrocnemius; LS:RS = left and right soleus. Based on observations of the full data set, we also determined that data from two muscle pair groups, i.e., LMG:RMG and LS:RS, would not be included in our final analyses due to insufficient apparent EMG connectivity.

2.4. Data Analysis

2.4.1. Signal Preprocessing

All data were low pass filtered at 450 Hz with a 4th order Butterworth filter to isolate EMG activity. A 60 Hz, 2nd order Butterworth notch filter with a 0.2 Hz bandwidth was implemented to remove power line interference. Since power line noise exists in the middle of the gamma frequency band, we split the gamma band around this distortion into lower and upper gamma. We also ignored the delta and theta bands because of their susceptibility to motion artifacts. The 0-20 Hz frequency range is known to contain noise due to motor unit firing (0-20 Hz) and skin conductance (0-1 Hz). These sources of noise overlap with the frequency contents of the alpha and part of the beta bands.

Finally, the EMG signals were filtered into alpha (8-13 Hz), beta (13-30 Hz), lower gamma (30-60 Hz), and upper gamma (60-100 Hz) neural frequency band ranges using a 4th order Butterworth filter. Filtered data from each frequency band was retained for subsequent MI estimation.

2.4.2. Estimation of MI

MI was estimated using MATLAB toolbox Mutual Information Distance and Entropy Reduction (MIDER), a method for inferring network structures with information theoretic concepts [66]. MIDER estimates the probability distribution using the adaptive binning method described by Cellucci et al. [67].

MI was estimated between nine muscle pairs (Table 5), and computed over two-second segments (2400 data points) with 25% overlap between adjacent segments for a total of 19 segments per data record. Each segment was windowed using a Hamming window and the average MI of the 19 segments was used across each much pair, frequency band, standing condition, for each participant. Mutual information was normalized using the scale from 0 to 1 within each of the 19 segments using the method described in MIDER as Michaels [67]

$$I_{N_M}(X,Y) = \frac{I(X,Y)}{\max\left(H(X)H(Y)\right)},$$

where MI is normalized in the 0 to 1 range based on the maximal entropy of each contributing time series *[x]*. A functional block diagram for data and statistical analysis is illustrated in Figure 1.

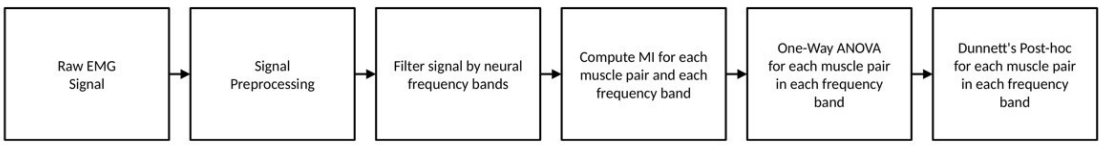

Figure 1. Steps for data processing for each of five trials and six test conditions for each participant.

 doi:10.20944/preprints202604.0137.v1

2.5. Statistical Analysis

Statistical analysis and graphics were performed with R Statistical Software (v4.4.0; R Core Team 2024) [68] running in RStudio: Integrated Development Environment for R [69]. Average normalized MI estimates for each set of five independent trials across the six test conditions within the seven muscle pairs and four frequency bands for each participant were examined.. The resulting charts for each of the six participants are included in Appendix B, with only participant #3 (PO3) data included in Section 3.1 (Figure 2). A single graphic (Figure 9) with all data from this reduced set of data was generated to help visualize inter-trial and inter-participant variation. Analysis was done on 168 sets of thirty MI values from the six conditions and five independent trials within each participant, frequency band, and muscle group. The primary goal of the analysis was to determine under what conditions the mean normalized MI differed from the baseline EOFT condition using a Dunnett's test. Assumptions of normality (Shapiro tests) and homogeneity of variance (Levene's test) were performed on each data set with failures of assumptions graphed using Q-Q plots and boxplots. Given the exploratory nature of this study and the mild nature of deviations from the statistical assumptions, we chose to apply parametric methods without transformation for simplicity. Dunnett's test results are summarized graphically with an array of 95% Dunnett's confidence interval charts (Figure 3 – Figure 8) each showing the interval for the mean difference between the less stable condition (ECFT, EOTanDB, ECTanDB, EOTanDF, and ECTanDF) and the baseline EOFT condition, i.e., the interval for the increase in normalized MI for each of the less stable conditions. Intervals associated with a significant (p-value < 0.05) are colored blue. Note: ANOVA F-tests were performed but rejected too frequently, i.e., a significant F-test often did not result in any significant Dunnett's intervals. This is because the F-test looks at all possible pairs of conditions, not just the five comparisons of interest but all 15 possible combinations.

Having both MI and MSC [39] results available for each participant and trial allowed a direct comparison of the two similarity measures. Theoretically, MI should detect non-linear similarities between EMG sequences that MSC could not. The nature of biological systems suggest that such non-linear characteristics should be present. This comparison was performed with a simple linear model attempting to predict MI from MSC. If only linear similarity existed, the two measures should have a linear relationship. Nonlinearity would be an indication of MI detecting information not picked up by MSC. A linear model of MI as a function of MSC and frequency band allowing for separate intercepts, slopes and quadratic terms for each frequency band was fit and illustrated graphically in Figure 10.

3. Results

3.1. Overview of MI Across Participants

We focused the analysis of the MI for each muscle pair and all participants across the test conditions and in the alpha, beta, lower gamma, and upper gamma frequency bands. This section will include an overview of the MI patterns across participants, based on observation. Because of the variability of the MI data (details to be discussed in Section 3.3) we will not show overall patterns from a representative participant. Instead, we will provide the MI from participant #3 (P03) to assist the reader in their review of all participant data, which can be found in Appendix B.

Our qualitative analysis noted the following MI patterns (Figure 2):

- Greater normalized MI between muscle pairs in the tandem stance compared to the feet together positions in the beta, lower gamma, and upper gamma frequency bands;
- Consistently greater normalized MI in the LMG:LS and RMG:RS in the beta, lower gamma, and upper gamma frequency bands for tandem stance positions under eyes open and eyes closed conditions;
- Evidence of MI between antagonistic muscle pairs, particularly LTA:LS, RTA:RMG, and RTA:RS; and

 doi:10.20944/preprints202604.0137.v1

- No distinguishable MI patterns in the tandem standing positions with the dominant leg positioned back or forward.

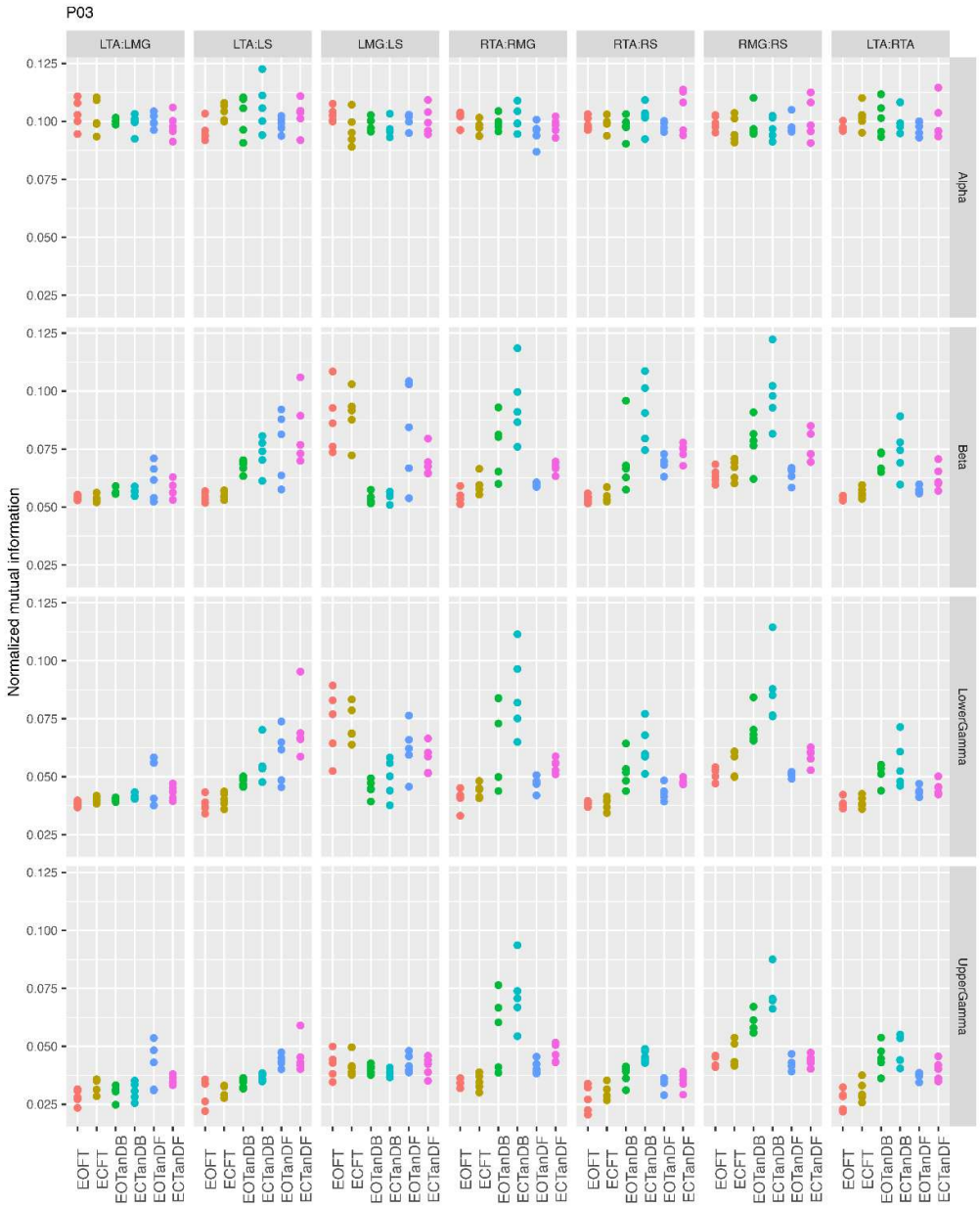

Figure 2. MI for participant #3 (P03) for five trials over six conditions (EOFT = eyes open feet together; ECFT – eyes closed feet together; EOTanDB = eyes open tandem dominant leg back; ECTanDB = eyes closed tandem dominant leg back; EOTanDF = eyes open tandem dominant leg forward; ECTanDF = eyes closed tandem dominant forward) for muscle pairs across four frequency bands: alpha (8-13 Hz), beta (13-30 Hz), lower gamma (30-60 Hz), and upper gamma (60-100 Hz). Note: LMG:RMG = left and right medial gastrocnemius; LS:RS = left and right soleus; LTA:RTA = left and right tibialis anterior.

3.2. Comparison of MI Across Conditions

One of our purposes was to examine whether MI differed between a baseline standing posture (defined as eyes open feet together [EOFT]) and less stable standing postures, e.g., tandem standing position with eyes open and closed. A Dunnett's inferential analysis demonstrated differences in the

 doi:10.20944/preprints202604.0137.v1

MI between more and less stable standing postures across select muscle pairs and test conditions. In this section, we will show data from all six participants and highlight the major findings.

Common findings in all participants included:

- More significant differences in MI between tandem standing and the baseline standing positions in the beta, lower gamma, and upper gamma frequency bands;
- Greater normalized MI in tandem standing for select muscle pairs, but particularly lower leg synergists, i.e., medial gastrocnemius/soleus;
- Greater normalized MI in the left tibialis anterior/right tibialis anterior in tandem standing, consistently across the beta, lower gamma, and upper gamma frequency bands.

Participant #1 (P01) demonstrated a consistent difference in MI values between the baseline and tandem standing (dominant leg back) positions, with greater MI for the RMG:RS muscle pair across all frequency bands. However, for the LMG:LS muscle pair there was greater normalized MI in tandem standing with the dominant leg forward. P01 demonstrated no differences in MI across all frequency bands and test conditions for the LTA:LMG muscle pair, but showed greater MI in tandem standing with the antagonistic LTA:LS muscle pair in the beta and lower and upper gamma frequency bands (Figure 3).

 doi:10.20944/preprints202604.0137.v1

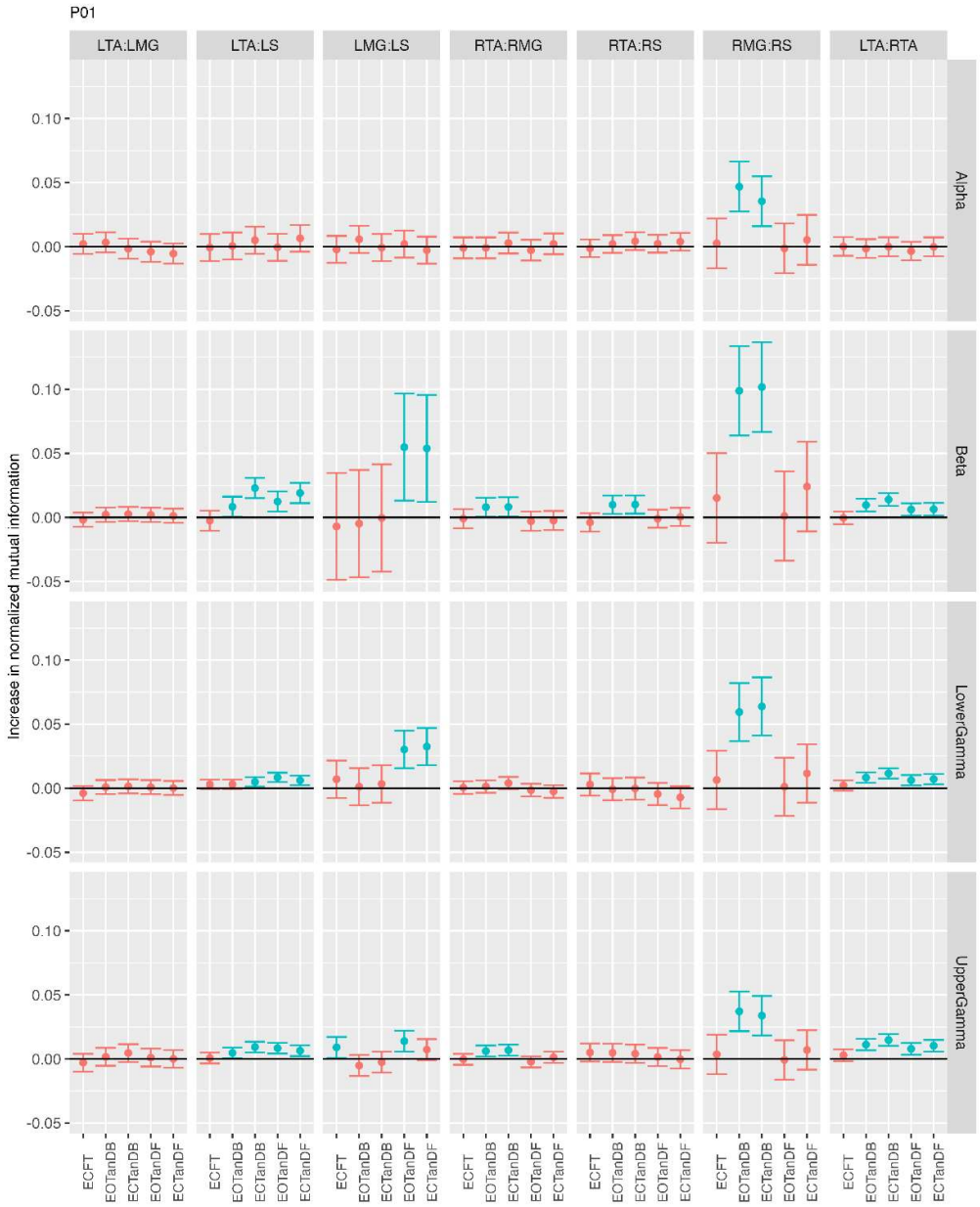

Figure 3. Confidence intervals (CIs) for mean differences in normalized mutual information between the baseline (EOFT) and less stable, e.g., EOTanDB, standing positions for P01. Differences and their CIs are presented as red (no significant difference) and blue (significantly different). The black horizontal line indicates zero difference, CIs above zero indicate that the test condition was greater than the baseline, and CIs below zero indicate that the test condition was less than the baseline.

Like P01, participant #2 showed no differences in MI between the baseline and less stable standing positions for the LTA:LMG muscle pair across all frequency bands and test conditions, and similar patterns of increased MI for the LTA:LS muscle pair in the beta and lower gamma frequency bands for the less stable postures. P02 demonstrated larger MI differences in the LMG:LS than the RMG:RS muscle pairs in tandem standing, but appeared to have variable MI differences when standing in tandem with the dominant leg back or forward (Figure 4).

 doi:10.20944/preprints202604.0137.v1

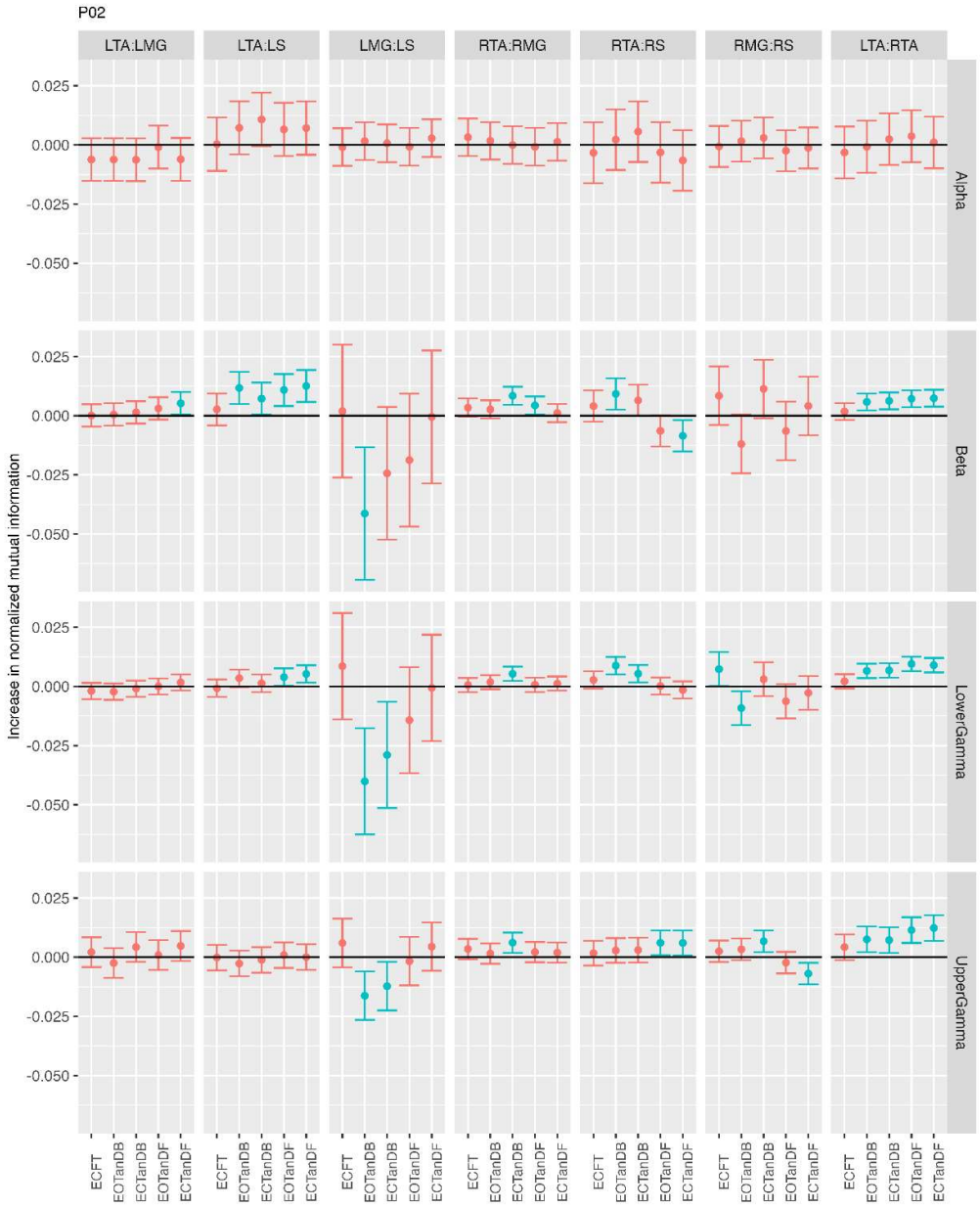

Figure 4. Confidence intervals (CIs) for mean differences in normalized mutual information between the baseline (EOFT) and less stable, e.g., EOTanDB, standing positions for P02. Differences and their CIs are presented as red (no significant difference) and blue (significantly different). The black horizontal line indicates zero difference, CIs above zero indicate that the test condition was greater than the baseline, and CIs below zero indicate that the test condition was less than the baseline.

Similar to P02 but unlike P04, P03 (Figure 5) demonstrated no differences in normalized MI across all muscle pairs and conditions in the alpha frequency band. However, unlike the first two participants, P03 and P04 (Figure 6) showed more and greater normalized MI values across all muscle pairs in the beta and lower and upper gamma frequency bands. Furthermore, evidence of increased MI was observed in tandem standing in both the dominant leg back and forward positions.

 doi:10.20944/preprints202604.0137.v1

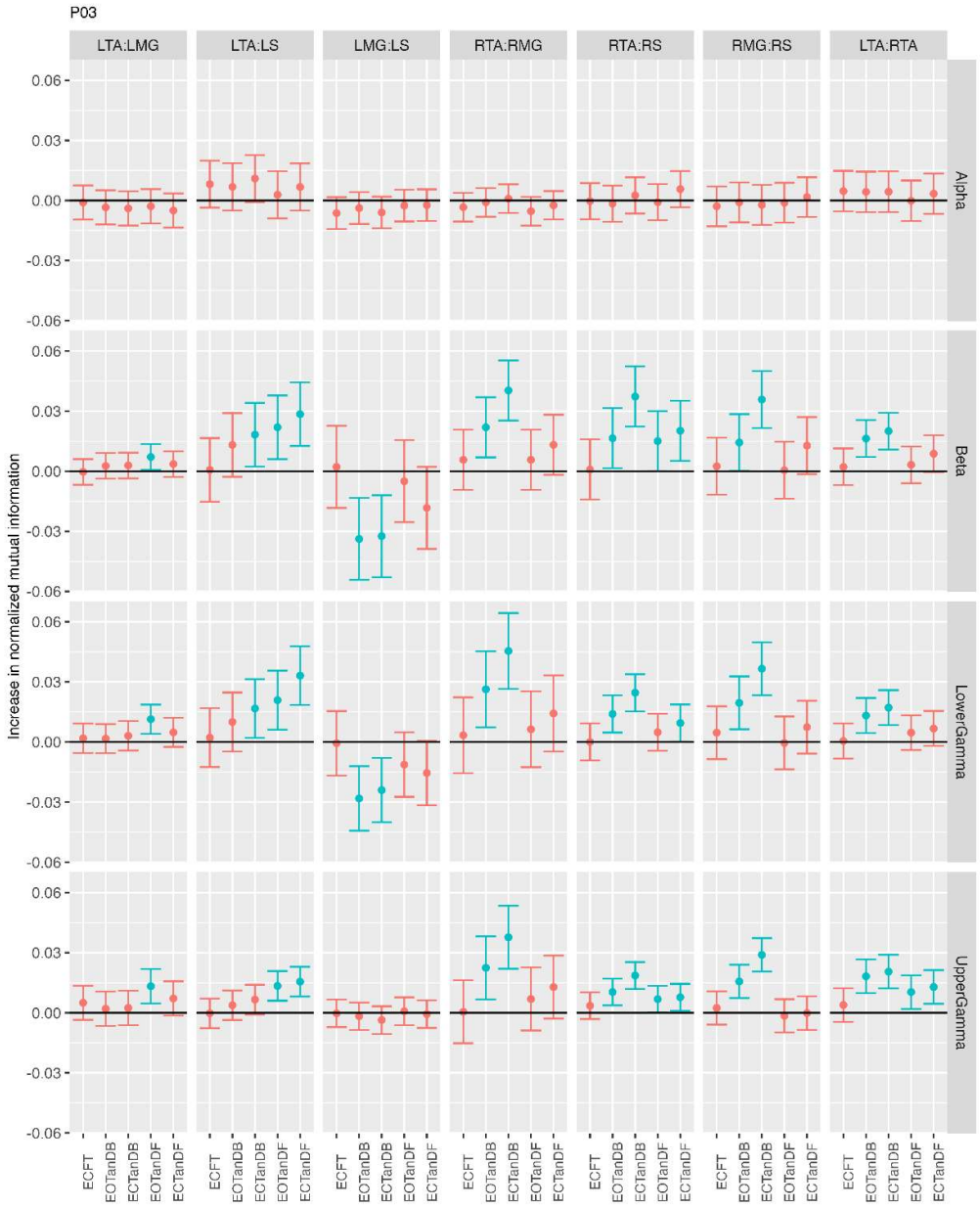

Figure 5. Confidence intervals (CIs) for mean differences in normalized mutual information between the baseline (EOFT) and less stable, e.g., EOTanDB, standing positions for P03. Differences and their CIs are presented as red (no significant difference) and blue (significantly different). The black horizontal line indicates zero difference, CIs above zero indicate that the test condition was greater than the baseline, and CIs below zero indicate that the test condition was less than the baseline.

 doi:10.20944/preprints202604.0137.v1

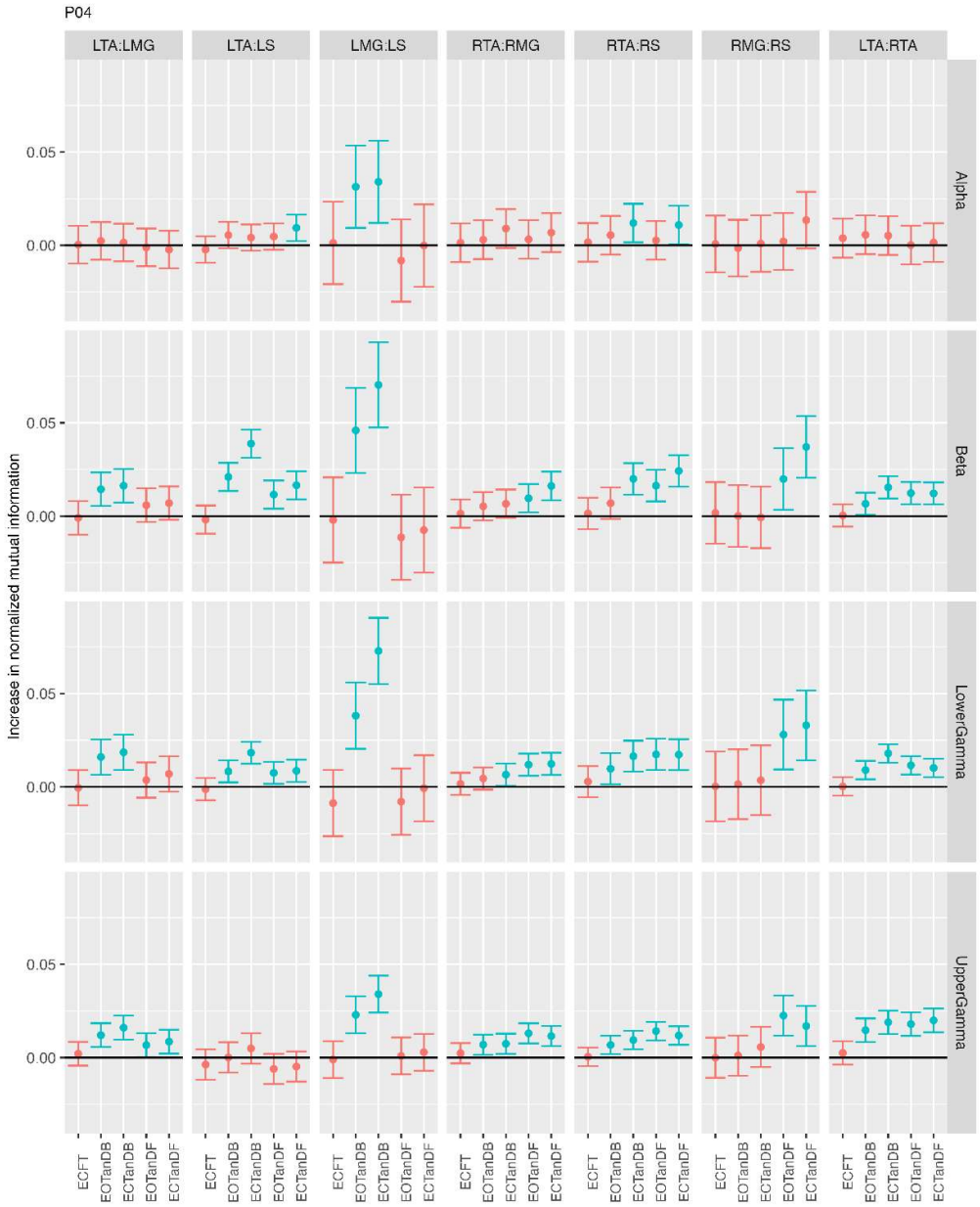

Figure 6. Confidence intervals (CIs) for mean differences in normalized mutual information between the baseline (EOFT) and less stable, e.g., EOTanDB, standing positions for P04. Differences and their CIs are presented as red (no significant difference) and blue (significantly different). The black horizontal line indicates zero difference, CIs above zero indicate that the test condition was greater than the baseline, and CIs below zero indicate that the test condition was less than the baseline.

Participants #5 (Figure 7) and #6 (Figure 8) both demonstrated variable increases in normalized MI in less stable standing positions in the alpha frequency band, but not for identical muscle pairs. Whereas P05 showed significant increased MI in the LTA:LMG muscle pair in the beta, and lower and upper gamma frequency bands in nearly all less stable standing positions, MI differences in the LTA:LMG muscle pair for P06 were negligible. Both P05 and P06 demonstrated large MI differences for the LMG: LS muscle pair across all frequency bands in tandem standing with the dominant leg back, and increased MI for the RMG:RS muscle pair in tandem standing with the dominant leg forward. Increased MI was also notable in the RTA:RS antagonistic muscle pair for both participants standing tandem with the dominant leg forward.

 doi:10.20944/preprints202604.0137.v1

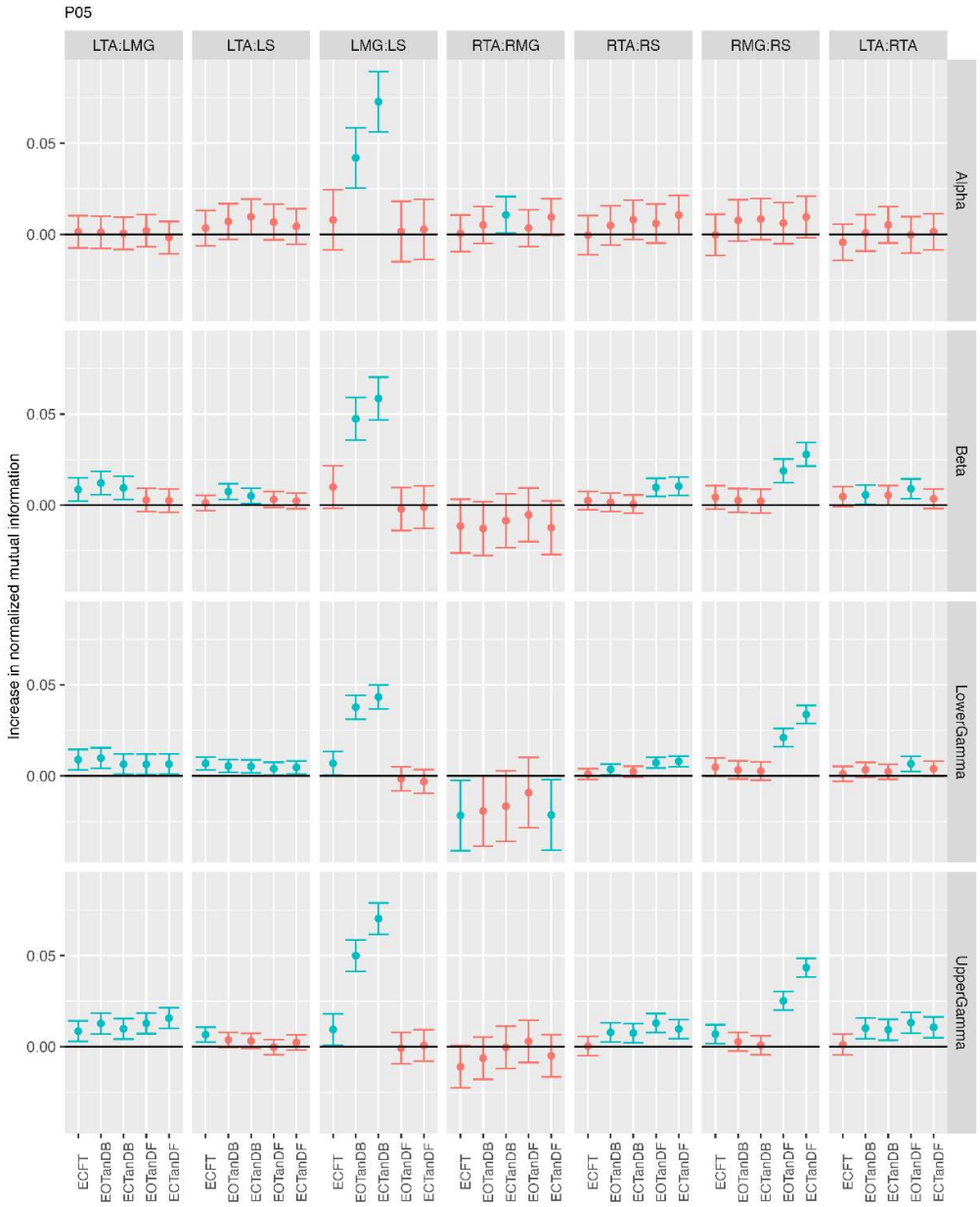

Figure 7. Confidence intervals (CIs) for mean differences in normalized mutual information between the baseline (EOFT) and less stable, e.g., EOTanDB, standing positions for P05. Differences and their CIs are presented as red (no significant difference) and blue (significantly different). The black horizontal line indicates zero difference, CIs above zero indicate that the test condition was greater than the baseline, and CIs below zero indicate that the test condition was less than the baseline.

 doi:10.20944/preprints202604.0137.v1

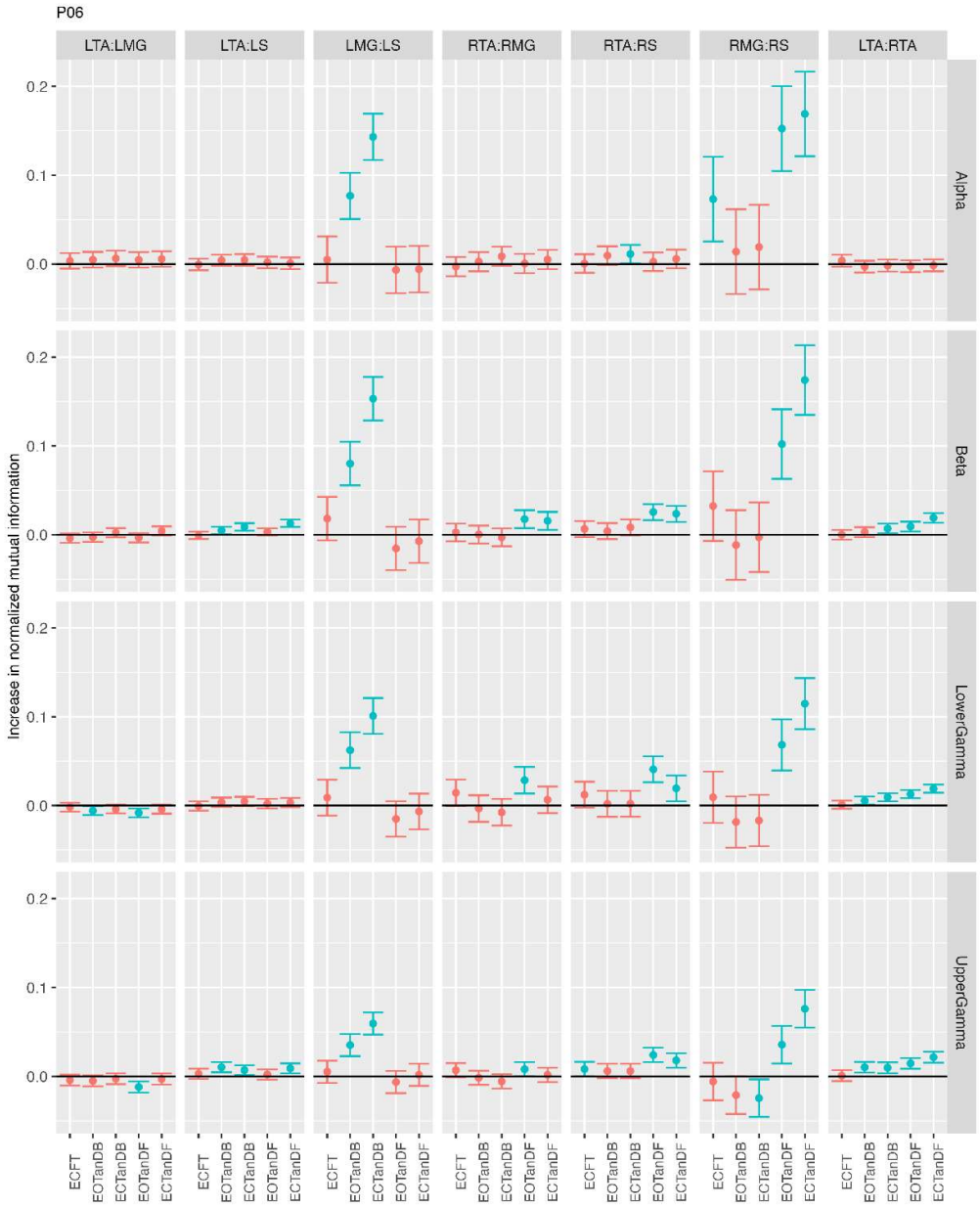

Figure 8. Confidence intervals (CIs) for mean differences in normalized mutual information between the baseline (EOFT) and less stable, e.g., EOTanDB, standing positions for P06. Differences and their CIs are presented as red (no significant difference) and blue (significantly different). The black horizontal line indicates zero difference, CIs above zero indicate that the test condition was greater than the baseline, and CIs below zero indicate that the test condition was less than the baseline.

In summary (from Sections 3.1 and 3.2), 1), generally there were notable differences between the six participants in how normalized MI values changed with tandem standing, whether the dominant leg was back or forward; 2) MI significantly increased in selected muscle pairs under tandem standing conditions; 3) the most common muscle pairs that saw significant MI changes with tandem standing were LMG:LS and RMG:RS; 4) increased MI associated with antagonistic muscle pairs, e.g., LTA:LS and muscle pairs on the contralateral leg, e.g., LTA:RTA suggests a more complex motor control pattern during less stable standing postures; 5) there did not appear to be a pattern of MI differences in the eyes open and closed conditions; and 6) there was no specific pattern to changes in normalized MI whether the dominant leg was back or forward in tandem standing.

 doi:10.20944/preprints202604.0137.v1

3.3. Inter-Trial and Subject Variability in Normalized MI

Previously, we identified the inter-trial and participant variability (Sections 3.1 and 3.2; see also Appendix B) in the normalized MI across the six participants. In Figure 9 we post the normalized MI for all trials and participants for each muscle pair across the four neural frequency bands, which clearly demonstrates this biological variability. It is clear that the greatest variability is seen in the LMG:LS and RMG:RS muscle pairs across all frequency bands. We think it notable that these same muscle pairs saw the greatest increase in normalized MI values under the tandem standing positions whether the dominant leg was back or forward. These results appear to support an intuition which might claim that this would be expected by these synergists. We also note that P06 showed the greatest inter-trial variability for the LMG:LS and RMG:RS muscle pairs.

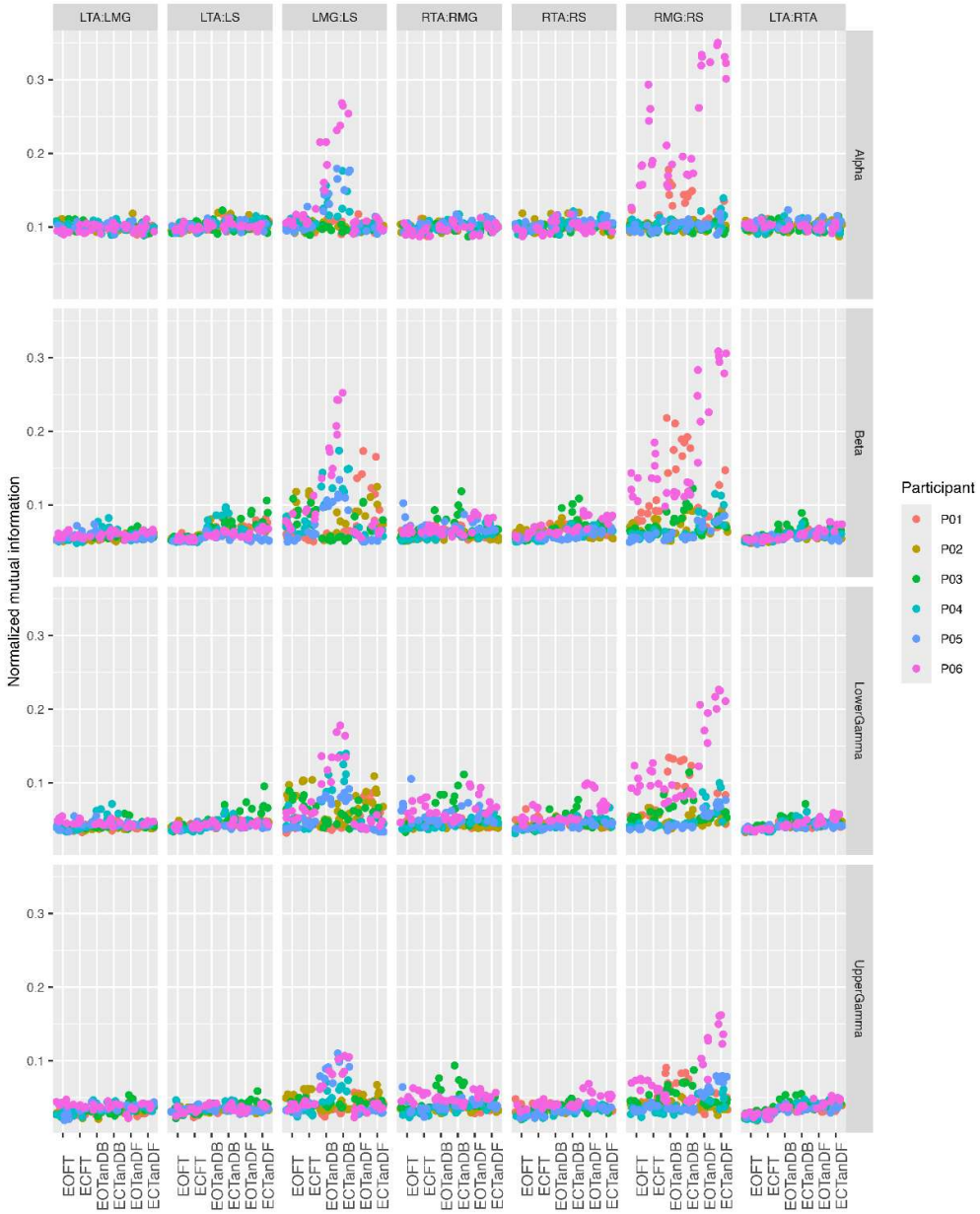

Figure 9. Normalized for all six participants across five trials, and all muscle pairs for the alpha, beta, and lower and upper gamma frequency bands.

3.4. Relationship Between MI and Magnitude-Sqaured Coherence

 doi:10.20944/preprints202604.0137.v1

Figure 10 illustrates the relationship between MI and MSC. The MSC results for our cohort have been previously published in [39]. The model fit lines clearly show a curvature indicating the presence of non-linearities being detected by MI that were not present in the MSC results. All coefficients except the alpha band slope were significant at the 0.05 level. The alpha band slope trended toward significance at p = 0.0556.

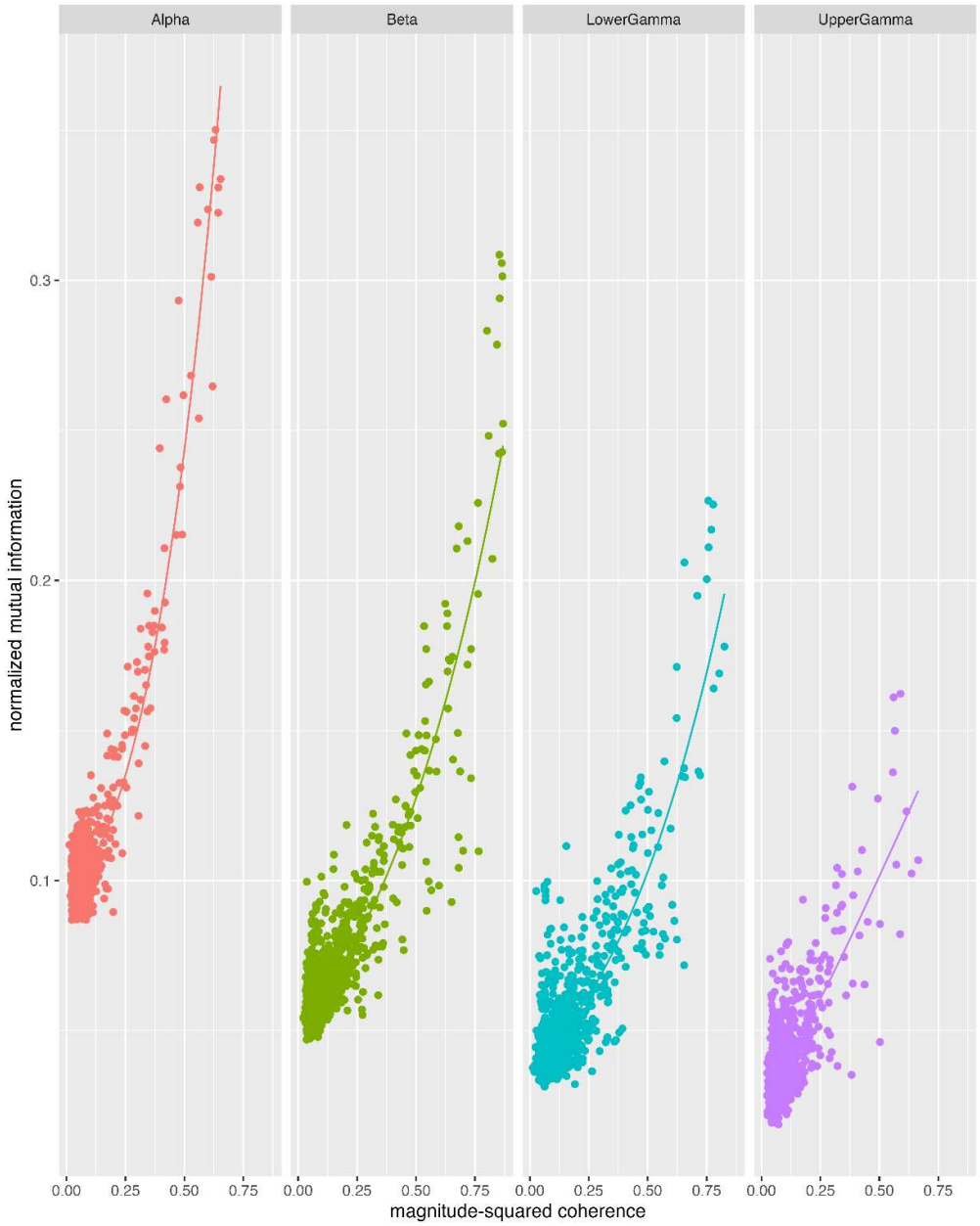

Figure 10. Plot of normalized MI with respect to MSC for all participants, muscle pairs, conditions, and trials with quadratic models showing curvature.

4. Discussion

We've noted the significant incidence of falls related to reduced ability to control static and dynamic balance [1,8] related to aging and neuropathology [2–7], and the need, therefore, to continue to acquire insight in the neuro-musculoskeletal mechanisms related to the control of standing balance. We previously reported that the EMG-EMG MSC for selected lower leg muscles was greater during tandem stance across different neural frequency bands, when compared to natural bipedal

 doi:10.20944/preprints202604.0137.v1

standing, providing some insight into the neural control of less stable standing postures [39]. This type of information gathered from both normal healthy adults have provided a baseline that can be used to aid in diagnosis, rehabilitative strategies, and in the longitudinal assessment of patients with impaired standing balance. Despite the significant insights into the possible origin of neuro-mechanical control of standing balance using traditional linear functions, like MSC, these methods are limited by their inability to account for the variability and complexity of the nonlinearity of time series datasets from dynamical systems.

MI is an information-theoretic measure that can quantify the total amount of shared information (both linear and nonlinear dependencies) between two signals, e.g., EMG of muscle pairs, that are coupled or coordinated under different standing balance conditions. That is, not only can MI assess inter-muscle coordination it can assist in the identification of neural control strategies across different neural frequency bands, as well as detect nonlinear dependencies between EMG signals, thus offering a more complete picture of complex muscle interactions and altered activation patterns. Therefore, the purpose of this project was to re-analyze the EMG data from our previous study [39] and describe how MI between muscle pairs may change with less stable standing positions, e.g., feet together vs. tandem stance, under eyes-open or closed conditions. Similar to our previous research [39], we found that normalized MI was greater, particularly in the medial gastrocnemius and soleus muscle pairs, across the beta, lower gamma, and upper gamma frequency bands in the tandem standing posture under both eyes open and eyes closed conditions. Although MI was typically greater in muscle pairs of the rear leg, leg dominance did not appear to be distinguishable during tandem standing. Finally, normalized MI generally increased in antagonistic muscle pairs, e.g., left tibialis anterior and soleus, in the less stable standing positions.

Bipedal quiet standing relies on the central nervous system (CNS) to coordinate multiple degrees of freedom (DoF) to provide stability and maintain balance [10,70–72]. Berstein [10,12,73] proposed a hierarchical control theory which suggested that the CNS governed the DoF problem using specific functional control entities. Although Latash and colleagues [70–72,74] acknowledged the variability in human movements and the challenges posed by multiple DoF, they understood that the CNS's capacity to organize numerous muscle and joints within a redundant system into functionally coherent actions could be explained. Rather than controlling each joint or muscle separately, the CNS was thought to stabilize key task outcomes that were essential for the successful execution of dynamic and static actions under a principle of abundance. This principle suggested that all of the elements, i.e., DoF, always participated in all tasks, such that the CNS did not eliminate redundancy but exploited it to allow for flexible and adaptive control strategies [14].

In the past 30 years, alternative uses of EMG datasets have emerged that examined the spectral information related to motor unit action potentials and motor neuron firing patterns [75,76]. It has been shown that presynaptic inputs to motor neuron pools of muscle pairs, or other combinations, can synchronize their firing frequency, where the strength of such synchronization is apparent in coherence measures; that is, measures of correlation in the frequency domain between trains of action potentials from motor neurons innervating two or more muscles. Thus, common neural inputs to different muscles can be inferred from their intermuscular coherence, which can then be used to define common neural drives that simultaneously activate motor pools related to functional synergies [49–55]. If meaningful information can be derived from discerning the common inputs, i.e., synchronized muscle activation, to functional muscle synergies, we may be able to advance our understanding of human movements and postural control [41,75,77,78].

Many previous studies have used inter-muscular coherence analysis across several neural frequency bands to examine standing postural control under a variety of conditions in young [22,33–38,40,77,82–87] and older adults [84–88]. During quiet standing, coherence of selected lower extremity muscles were reported in the 0-5 Hz (delta), 6-15 (alpha), and 13-30 Hz (beta) bands, reflecting subcortical [75,84] and corticospinal [89] input. It has been reported that when the standing task challenge increases corticospinal and subcortical inputs increases [36–39,91–93]. Research results indirectly germane to our work, i.e., EMG measures of lower leg muscles during tandem standing,

 doi:10.20944/preprints202604.0137.v1

came from [36–39]. Briefly, those authors reported comparable findings: 1) greater agonist-agonist, e.g., soleus-gastrocnemius, coherence compared to agonist-antagonist muscle pairs in all frequency bands (0-55 Hz); 2) greater coherence in the delta and lower gamma frequency bands for the agonist-agonist muscle pairs with increasing postural challenges, i.e., tandem standing with eyes closed; 3) greater coherence in the beta, and lower and upper gamma frequency bands for the LMG:LS and RMG:RS for tandem stance in both eyes open and closed conditions; and 4) no difference in coherence in muscle pairs when the dominant limb was placed in the back or fore position in tandem standing. Use of EMG-EMG coherence muscle pair analyses has shown that the neural signals to lower extremity muscles during normal quiet standing with increasing difficulty originates from several sources: corticospinal, brainstem, and subcortical/spinal. However, as noted earlier, these methods are limited by their inability to account for the variability and complexity of the nonlinearity of time series datasets from dynamical systems.

Several investigators [59–61,63] used MI in their analyses of quiet standing and only one [63] examined the sEMG of selected lower extremity muscles across multiple frequency bands in applying MI analyses of standing balance. Boonstra et al. [61,62] used a signal processing framework for the description of how information was processed by muscle networks and multivariate information decomposition of several lower and upper extremity muscles to examine their functional interactions under nine experimental conditions, including challenges to standing balance. They found that when posture was destabilized in the A/P direction, the number of connections between leg muscles was greatly enhanced, showing multiple edges between bilateral lower leg muscles and between upper and lower leg muscles. When posture was stabilized in the M/L direction, multiple connections were noted between the leg muscles and many more connections between leg and torso muscles. Results also showed that conditional transfer entropy, total transfer, and MI increased during A/P instability but were greatest under M/L instability conditions. Their results suggested that the correlated inputs related to the interactions they observed likely originated from supraspinal areas through divergent pathways or from presynaptic synchronization. O'Reilly et al. [63] measured the EMG of several lower extremity muscles during standing balance involving a reaching task and used MI in their analysis of intramuscular activation at several frequency bands: delta (0, 1-4 Hz), theta (4-8 Hz), alpha (8-12 Hz), beta (12-30 Hz), lower gamma (30-60 Hz), and upper gamma (60-80 Hz). They noted that poorer balance control correlated with inter-muscular activations, the gamma frequency data appeared to provide information to assist in the explanation of balance control, and motor variability among older adults may be explained by concurrent increases and decreases in the functional integration in inter- and intramuscular interactions.

There is no published research with which we can contrast to the specifics of our work. Therefore, based on the results of our previous research [39] and this project, we believe that there may be an interesting relationship between the EMG-EMG coherence and MI analyses of quiet standing in normal, healthy adults. Therefore, in this section, we will provide a qualitative comparison of the MSC and MI results for participant #3 (P03). Participant #3's MSC data graph (Figure 11) showed a consistent increase in coherence for muscle pairs in the tandem standing compared to the feet together standing conditions, with the greatest coherence changes in the LMG:LS and RMG:RS muscle pairs across the beta, lower gamma, and upper gamma frequency bands. Evidence of increased coherence between antagonistic muscle pairs, e.g., LTA:LS, during tandem standing suggests that co-actions of antagonists may increase ankle stiffness during less stable standing postures, and/or corroborative with Latash's principle of abundance [70,71]. There were no observable differences in muscle pair coherence between the eyes open and closed conditions or when P03 stood with the dominant leg in the back position or forward position during tandem standing. Similar results were found in the normalized MI data graph (Figure 3) for P03. However, there appeared to be greater MI differences in three agonist-antagonist muscle pairs, LTA:LS, RTA:RMG, and RTA:RS across all frequency bands, rather than just one, which was unique to P03 (see Appendix B). These findings suggest two possibilities. Firstly, MI may provide additionally unique data related to the activation of muscle synergies during the internal perturbation of quiet

 doi:10.20944/preprints202604.0137.v1

standing in normal healthy adults. Secondly, there appears to be a nonlinear relationship between MSC and normalized MI values across the neural frequency bands we studied (Figure 11). Additional research including a replication of our method with a larger cohort is needed to further explore these initial findings.

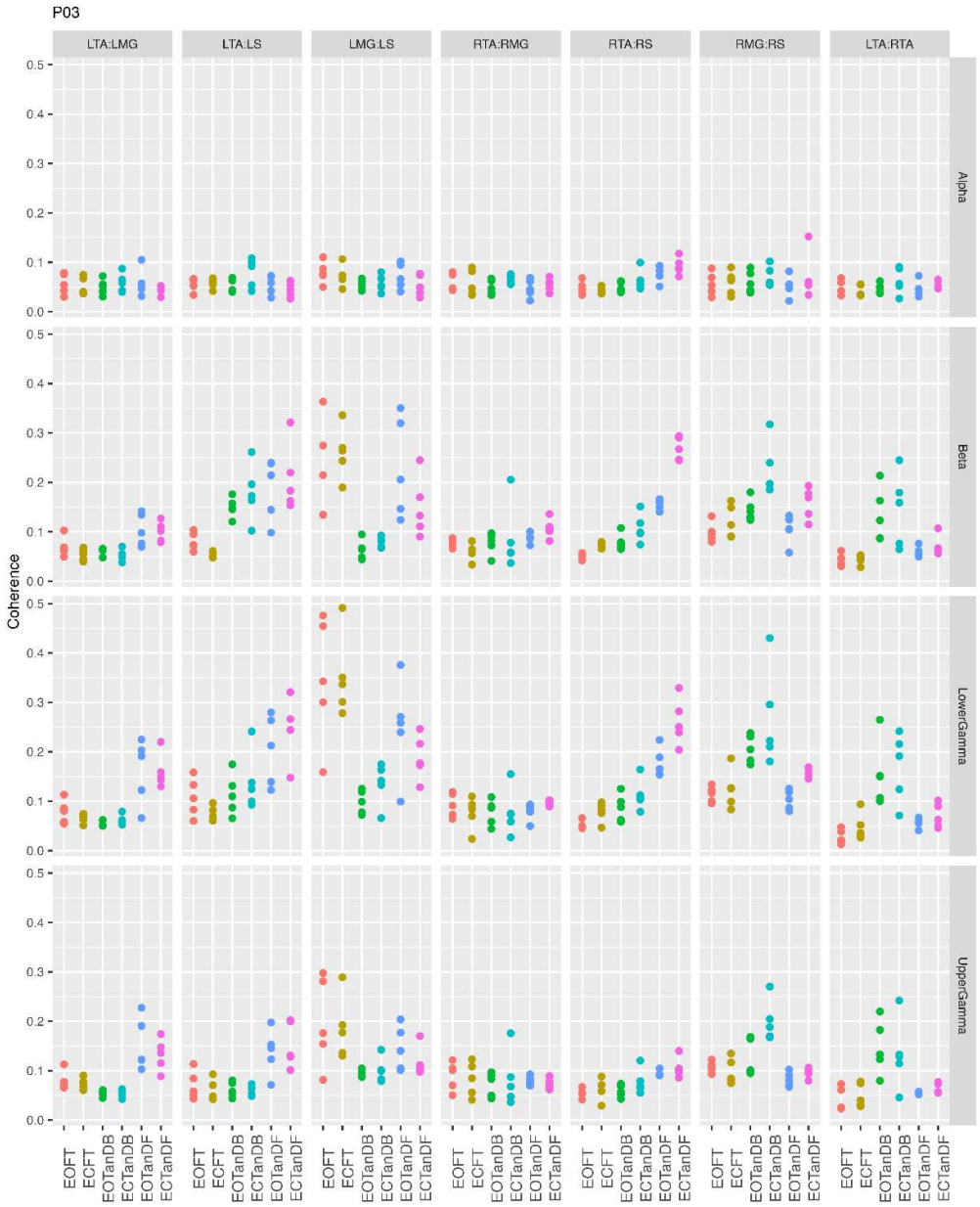

Figure 11. EMG-EMG muscular coherence for Participant #3 (P03) for five trials over six conditions (EOFT = eyes open feet together; ECFT = eyes closed feet together; EOTanDB = eyes open tandem dominant leg back; ECTanDB = eyes closed tandem dominant leg back; EOTanDF = eyes open tandem dominant leg forward; ECTanDF = eyes closed tandem dominant leg forward) for all muscle pair combinations across four frequency bands: alpha (8-13 Hz), beta (13-30 Hz), lower gamma (30-60 Hz), and upper gamma (60-100 Hz). Note: LMG:RMG = left and right medial gastrocnemius; LS:RS = left and right soleus; LTA:RTA = left and right tibialis anterior.

As we reported previously [39], there appeared to be notable inter-trial and inter-participant variability in normalized MI across our six participants, perhaps related to biological differences and the complexity of the motor control of the standing postures tested. Our findings are similar to those

 doi:10.20944/preprints202604.0137.v1

reported by Torres-Oviedo and Ting [21,94] and may also be indicative of the CNS's ability to use all elements in all postural tasks to ensure flexible responses to maintain standing balance [70,71].

As a type of statistical measure MI can quantify the linear and nonlinear dependence, i.e., amount of shared information, between discrete and continuous time series variables derived from complex dynamical systems. A unique feature of MI analyses, as compared to MSC analyses, rests in its derivation from entropy. In general, entropy analyses, e.g., approximate entropy, have been used to characterize biomechanical time series from complex systems, such as the CNS's control of standing postures in normal, healthy [95] adults and those with neuropathology [4]. A regular, more predicable process, i.e., system responses, produces reduced entropy values than a less regular ones [96,97]. Greater entropy values typify signals that are less predictable but may represent a normal CNS adaptable response to an unusual event, e.g., loss of balance. For example, Cavanaugh et al. [4] showed that, compared to healthy participants, post-concussed athletes exhibited lower, more regular approximate entropy values of antero-posterior (AP) and medio-lateral (ML) center of pressure time series collected during a standing postural task. This finding suggested that although the athletes had displayed normal postural stability the CNS had resorted to a less complex response. Previously, we used approximate and sample entropy methods to characterize the changes in the center of pressure excursions in the AL and ML directions under different standing conditions [98,99]. We found that both approximate (ApEn) and sample (SampEn) entropy values increased in both the AP and ML directions in three less stable (more difficult) standing positions, i.e., feet together eyes closed and tandem under eyes open and closed conditions. We concluded that the increased ApEn and SampEn values were consistent with a less predictable, more variable time series, but a normal response to a novel standing posture, e.g., tandem standing. We suggest that further research is needed to explore the unique interaction between entropy and the traditional view of the application of MI analyses related to the understanding of complex system's control, like human balance behavior.

4.1. Study Limitations

Future studies will need to employ larger cohorts and test individuals with individuals with a variety of musculoskeletal and neurological impairments. Unfortunately, because the raw EMG signals in this study were filtered we were unable to examine MI in the lower frequency band ranges, so future research should to re-examine this issue. On the other hand, we believe the fidelity of analysis of the other frequency band ranges was preserved. We did not examine our EMG for cross-talk although this was not likely an issue because the muscles we tested provided wide distinct surface areas. Despite the validation [13,100] of the single inverted pendulum model, others have suggested that a double inverted pendulum model may provide a more suitable framework to examine the complexity of quiet bipedal stance [101–103]. We agree that future research utilizing MI in the study of standing posture could include more lower extremity muscles as part of using a more complete and functional mechanical model. Although Winter et al. [15] demonstrated that the ankle invertor/evertor muscles were critical to the control of medio-lateral postural sway, we did not test the activity of any ankle evertors, e.g., peroneus longus. Future research using our protocol should include ankle invertor/evertor muscles and muscles from other muscle functional units known to control standing posture [19,20,22]. We defined leg dominance as the leg one would kick a ball with, yet there is no consensus in the literature on the definition of leg dominance. Since our test conditions were not randomly organized a learning effect may have biased our results. Although the MIDER package was convenient for estimating MI values, alternative estimation methods to determine mutual information, e.g., k-nearest neighbor estimation [42], should be considered in future research since it appears to be more accepted when working with continuous signals.

5. Conclusions

The major strength of our work lies in its successful attempt to fill the gap in the literature on the use of MI analysis of quiet pedal standing. We believe that the use of MI analyses may provide

 doi:10.20944/preprints202604.0137.v1

additional insights into how the CNS controls the multi-segmented musculoskeletal system under a variety of quiet standing postures for two reasons: 1) its ability to quantify the functional connectivity, i.e., total amount of shared linear and nonlinear dependencies, and coordination between two or more EMG signals from lower extremity muscles, and 2) its basis in entropy and ability to help understand the direction of information flow. The results of our MI analyses have contributed additional evidence that the CNS can implement a common neural drive to simultaneously synchronize and activate key ankle muscles needed to maintain postural stability during internal perturbations, e.g., tandem stance with eyes closed. Our results suggest that shared neural drives and muscle information in the beta and lower and upper gamma frequency ranges may be related to the control of tandem standing. Additionally, it appears that functional muscle synergies are more important than simply limb dominance, although our data corroborate earlier studies that showed that in tandem standing greater muscle activity occurs in the rear leg. Our MI analysis provided evidence to identify changes in antagonistic or bilateral homologous connectivity with increasing instability. Finally, the inter-trial and participant variability appears to be consistent with the principle of abundance suggesting that formal information theory analysis of these data may be warranted. Our results suggest that clinical testing of tandem balance tasks might be a useful adjunct to the clinical measure of balance for individuals with musculoskeletal and neurological impairments.

Author Contributions: Conceptualization, DM, SR, GA; Methodology, DM, SR, GA; Software, DM, DWZ; Validation, DM; Formal Analysis, DM, SR, GA, DWZ; Resources, GA; Data curation, DM, SR; Writing (original draft) – DM; Writing (review and editing), DM, SR, GA, DWZ; Visualization, DM, SR, DWZ; Supervision, SR, GA, DWZ; Project administration, SR, GA; All authors have read and agreed to the published version of the Manuscript.

Funding: This research received no external funding.

Institutional Review Board Statement: The study was conducted following the Declaration of Helsinki and approved by the Institutional Review Board of Grand Valley State University(18-246-H) for studies involving humans.

Informed Consent Statement: Informed consent was obtained from all subjects involved in the study.

Data Availability Statement: The data presented in this study are available on request from the corresponding author due to restrictions imposed by our institution on retired faculty.

Acknowledgments: We acknowledge University administrative support for the use of equipment and materials needed for motion capture in the Biomechanics and Motor Performance Laboratory and all study participants.

Conflicts of Interest: The authors declare no conflicts of interest.

Appendix A. Mutual Information Theory

This appendix will provide a somewhat more detailed view of entropy and mutual information. Considerably more detail and proofs can be found in Chapter 2 of the Cover and Thomas' text [47].

A common way of illustrating entropy and mutual information is a Venn diagram like Figure A1. The circles in the entropy diagram depict uncertainty or information. The entirety of the information is the two circles with some of that information shared between the two. This is the mutual information, $I(X;Y)$.

 doi:10.20944/preprints202604.0137.v1

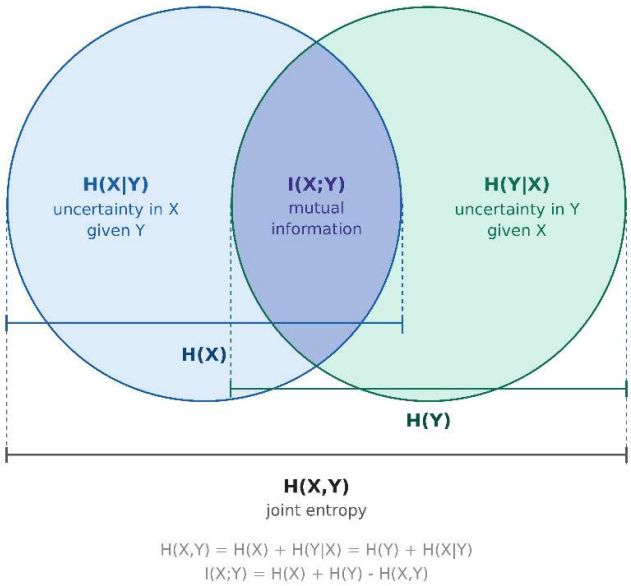

Figure A1. Venn diagram for entropy and MI. Drawings created using Claude.ai.

If X can take the values $\{x_1, \ldots, x_n\}$ and $p(x)$ is the probability associated with values given $x \in X$, entropy is defined as:

$H(X) = -\sum_{x \in X} p(x) \log p(x)$,

where logarithm of base 2 is the usual choice. Entropy is not affected by zero probability events since $lim_{x \to 0} \cdot log_2(x) = 0$; thus, since $0 \leq p(x) \leq 1$, $H(x)$ is strictly positive. For continuous $p(x)$, the summation is replaced with integration. Note that entropy is based on the probability of occurrence of each symbol; that is, entropy is not a function of the values of a series but a function of their probabilities [82]. The magnitude of $H(X)$ is then the average or expected information of an event.

$$H(X) = -E_{p(x)} \log (p(x))$$

Since entropy, as defined above, is relative to a single random variable it must be extended to a pair of random variables to get mutual information. The joint entropy $H(X,Y)$ of a pair of discrete random variables (X,Y) with a joint distribution $p(x,y)$ is defined as follows:

$H(X,Y) = -\sum_{x \in X} \sum_{y \in Y} p(x,y) \log p(x,y)$,

also, expressed as an expectation

$H(X,Y) = -E_{p(x,y)} \log p(x,y)$,

where the expectation is over $p(x,y)$.

Conditional entropy of X given Y is defined as the expectation over $p(x,y)$ of the log of the conditional probability of X given Y,

$H(X \mid Y) = -E_{p(x,y)} log(p(x|y))$.

Mutual information (MI) is a measure of the amount of information that one random variable contains about another random variable, which reduces the uncertainty of one random variable due to the knowledge of the other [80]. We define mutual information, $I(X;Y)$ as the relative entropy between the joint distribution and the product distribution $p(x)p(y)$,

$I(X;Y) = \sum_{x,y} p(x,y) log \frac{p(x,y)}{p(x)p(y)}$,

where $p(x,y)$ is the joint probability distribution for the occurrence of joint state (x, y) and $p(x)$ and $p(y)$ are the marginal probability distributions of X and Y, respectively. Mutual information is also an expectation:

$$I(X;Y) = E_{p(x,y)} log \frac{p(x,y)}{p(x)p(y)}$$

 doi:10.20944/preprints202604.0137.v1

In order to get the relationship between mutual information and entropy, we need relative entropy which is a measure of the distance between two distributions; a measure of the inefficiency of assuming that the distribution is q when the true distribution is p. Relative entropy, or the Kullback-Leibler distance between two probability mass functions $p(x)$ and $q(x)$ is defined as:

$D(p||q) = \sum_{x \in X} p(x) log \frac{p(x)}{q(x)}$.

$= E_{p(x)} log \frac{p(X)}{q(X)}$,

the expectation over p(x) of the log-probability ratio between distributions.

It can be assumed that relative entropy is always nonnegative and zero if and only if $p = q$. However, relative entropy is not a true distance since it is not symmetric $D(p||q) \neq D(q||p)$ and does not satisfy the triangle inequality.

Using the Kullback-Leibler distance, we get the relationship between mutual information and various entropy quantities illustrated in Figure A1.

$$I(X;Y) = I(Y;X)$$

$$I(X;Y) = H(X) - H(X|Y)$$

$$I(X;Y) = H(Y) - H(Y|X)$$

$I(X;Y) = H(X) + H(Y) - H(X,Y)$,

i.e., $I(X;Y)$ is the reduction in the uncertainty of X due to the knowledge of Y [80–82].

Appendix B

MI for each participant: five trials, over six test conditions (EOFT = eyes open feet together; ECFT = eyes closed feet together; EOTanDB = eyes open tandem dominant leg back; ECTanDB = eyes closed tandem dominant leg back; EOTanDF = eyes open tandem dominant leg forward; ECTanDF = eyes closed tandem dominant leg forward, for all muscle pair combinations (LMG/RMG = left/right medial gastrocnemius; LS/RS = left/right soleus; LTA/RTA = left/right tibialis anterior), and across four frequency bands: alpha (8-13) Hz, beta ([13-30 Hz), lower gamma (30-60 Hz), upper gamma (60-100 Hz).

 doi:10.20944/preprints202604.0137.v1

Figure A2. Normalized MI for participant#1 (P01).

 doi:10.20944/preprints202604.0137.v1

Figure A3. Normalized MI for participant#2 (P02).

 doi:10.20944/preprints202604.0137.v1

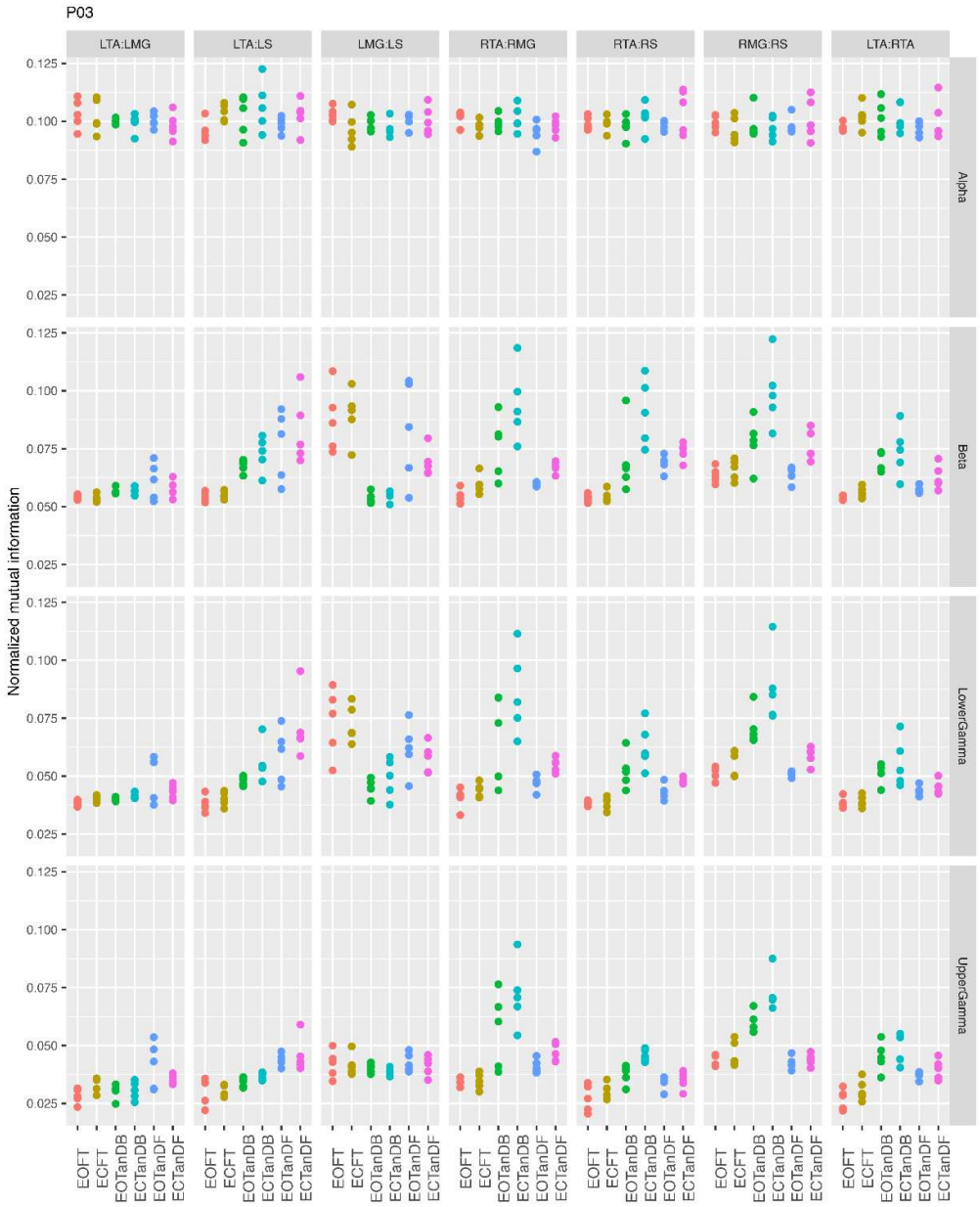

Figure A4. Normalized MI for participant#3 (P03).

 doi:10.20944/preprints202604.0137.v1

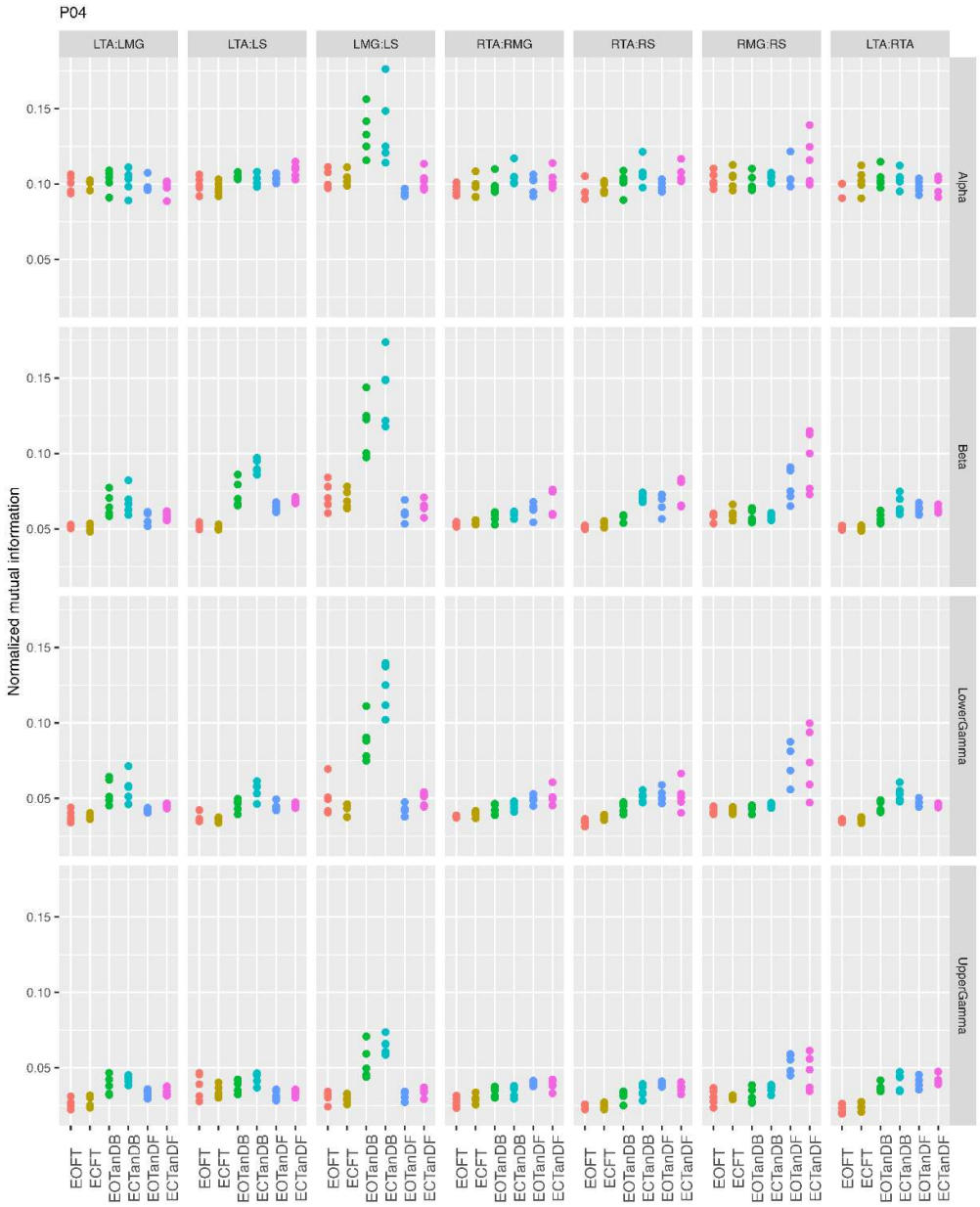

Figure A5. Normalized MI for participant#4 (P04).

 doi:10.20944/preprints202604.0137.v1

Figure A6. Normalized MI for participant#5 (P05).

 doi:10.20944/preprints202604.0137.v1

Figure A7. Normalized MI for participant#6 (P06).

References

1. Roman-Liu, D.; Age-related changes in the range and velocity of postural sway. *Arch Gerontol Geriatr.* **2018**, 77, 68-80. https://doi.org/10.1016/j.archger.2018.04.007.
2. Lamont, R.M.; Morris, M.E., Menz, H.B., McGinley, J.L., Brauer, S.G. Falls in people with Parkinson's disease: a prospective comparison of community and home-based falls. *Gait Posture* **2017**, 55, 62-67. http://dx.doi.org/10.1016/j.gaitpost.2017.04.005.
3. De Lima, F.; Melo, G., Fernandes, D.A., Santos, G.M., Neto, F.R. Effects of total knee arthroplasty for primary knee osteoarthritis on postural balance: a systematic review. *Gait Posture* **2021**, 89, 139-160. https://doi.org/10.1016/j.gaitpost.2021.04.042.
4. Cavanaugh, J.T., Guskiewicz, K.M., Giuliani, C., Marshall, S., Mercer, V., Stergiou, N. Detecting altered postural control after cerebral concussion in athletes with normal postural stability. *Br J Sports Med*. **2005**, 39, 805-811. https://doi.org/10.1136/bjsm.2004.015909.

 doi:10.20944/preprints202604.0137.v1

5. Buckley, T.A., Oldham, J.R., Caccese, J.B. Postural control deficits identify lingering post-concussion neurological deficits. *J Sport Health Sci*. **2016**, 5, 61-69. https://doi.org/10.1016/j.jshs.2016.01.007.
6. Weerdesteyn, V.; de Niet, M., van Duijuhoven, H.J.R., Geurts, A.C.H. Falls in individuals with stroke. *J Rehabil Res Dev*. **2008**, 45(8), 1195-1214. DOI: 10.1682/JRRD.2007.09.0145.
7. Ambrose, A.F.; Paul, G., Hausdorff, J.M. Risk factors for falls among older adults: a review of the literature. *Maturitas* **2013**, 75, 51-61. http://dx.doi.org/10.1016/j.maturitas.2013.02.009.
8. Salari, N.; Darvishi, N., Ahmadipanah, M., Shohaimi, S., Mohammadi, M. Global prevalence of falls in older adults: a comprehensive systematic review and meta-analysis. *J Orthop Surg Res.* **2022**, 17, 334. https://doi.org/10.1186/s13018-022-03222-1.
9. Sporns, O.; Chialvo, D.R., Kaiser, M., Hilgetag, C.C. Organization, development and function of complex brain networks. *Trends Cogn Sci.* **2004**, 8(9), 418-425. doi:10.1016/j.tics.2004.07.008.
10. Berstein, N. *The Coordination and Regulation of Movements*, 1st ed., Pergamon Press Ltd., Oxford, UK, **1967**.
11. Wang, Z.; Ko, J.H., Challis, J.H., Newell, K.M. The degrees of freedom problem in human standing posture: collective and component dynamics. *PloS One* **2014**, 9(1), e85414. doi: 10.1371/journal.pone.0085414.
12. Bruton, M.; O'Dwyer, N. Synergies in coordination: a comprehensive overview of neural, computational, and behavioral approaches. *J Neurophsyiol.* **2018**, 120(6), 2761-2774. doi: 10.1152/jn.00052.2018.
13. Winter, D.A.; Prince, F., Stergiou, P., Powell, C. Medial-lateral and anterior-posterior responses associated with centre of pressure changes in quiet standing. *Neursci Res Comm.* **1993**, 12(3), 141-148.
14. Winter, D. Human balance and posture control during standing and walking. *Gait Posture* **1995**, 3(4), 193-214. https://doi.org/10.1016/0966-6362(96)82849-9.
15. Winter, D.A.; Prince, G., Frank, J.S., Powell, C., Zabjek, K.F. Unified theory regarding A/P and M/L balance in quiet stance. *J Neurophysiol.* **1996**, 75(6), 2334-2343. doi: 10.1152/jn.1996.75.6.2334.
16. Winter, D.A.; Patla, A.E., Prince, F., Ishac, M., Krystyna, G.-P. Stiffness control of balance in quiet standing. *J Neurophysiol.* **1998**, 80, 1211-1221. doi: 10.1152/jn.1998.80.3.1211.
17. Winter, D.A.; Patla, A.E., Ishac, M., Gage, W.H. Motor mechanisms of balance during quiet standing. *J Electromyogr Kinesiol*. **2003**, 13, 49-56. doi: 10.1016/s1050-6411(02)00085-8.
18. Warnica, M.J.; Weaver, T.B., Prentice, S.D., Laing, A.C. The influence of ankle muscle activation on postural sway during quiet stance. *Gait Posture* **2014**, 39(4), 1115-1121. doi: 10.1016/j.gaitpost.2014.01.019.
19. Krishnamoorthy, V.; Goodman, S., Zatsiorsky, V. Latash, M.L. Muscle synergies during shifts of the center of pressure by standing persons: identification of muscle modes. *Biol Cybern.* **2003**, 89, 152-161. Doi: 10.1007/s00422-003-0419-5.
20. Krishnamoorthy, V.; Latash, M.L., Scholz, J.P., Zatsiorsky, V.M. Muscle synergies during shifts of the center of pressure by standing persons. *Exp Brain Res.* **2003**,152(3), 281-292. https://doi.org/10.1007/s00221-003-1574-6.
21. Torres-Oviedo, G.; Ting, L.H. Muscle synergies characterizing human postural responses. *J Neurophysiol.* **2007**, 98, 2144-2156. Doi:10.1152/jn.01360.2006.
22. Boonstra, T.W.; Danna-Dos-Santos, A., Xie, H., Roerdink, M., Stins, J.F., Breakspear, M. Muscle networks: connectivity analysis of EMG activity during postural control. *Sci Rep*. **2016**, 5, 17830. doi: 10.1038/srep17830.
23. Tanabe, H.; Fujii, K., Kouzaki, M. Intermittent muscle activity in the feedback loop of postural control system during natural quiet standing. *Sci Rep*. **2017**, 7(1), 10631. Doi:10.1038/s41598-017-10015-8.
24. Ting, L.H.; McKay, J.L. Neuromechanics of muscle synergies for posture and movement. *Curr Opin Neurobiol.* **2007**, 17(6), 622-628. Doi:10.1016/j.conb.2008.01.002.
25. Grosse, P.; Cassidy, M.J., Brown, P. EEG-EMG, MEG-EMG and EMG-EMG frequency analysis: physiological principles and clinical applications. *Clin Neurophysiol.* **2002**, 113(10), 1523-1531. doi: 10.1016/s1388-2457(02)00223-7.
26. Boonstra, T.W. The potential of corticomuscular and intermuscular coherence for research on human motor control. *Front Hum Neurosci.* **2013**, 7-2013. Doi:10.3389/fnhum.2013.00855.
27. Farina, D.; Negro, F., Dideriksen, J.L. The effective neural drive to muscles is the common synaptic input to motor neurons. *J Physiol.* **2014**, 592 (Pt 16), 3427-3441. doi: 10.1113/jphysiol.2014.273581.

 doi:10.20944/preprints202604.0137.v1

28. Farina, D.; Merletti, R., Enoka, R.M. The extraction of neural strategies from the surface EMG: an update. *J Appl Physiol.* **2014**, 117(11), 1215-1230. doi: 10.1152/japplphysiol.00162.2014.
29. Hug, F.; Del Vecchio, A., Avrillon, S., Farina, D., Tucker, K. Muscles from the same muscle group do not necessarily share common drive: evidence from the human triceps surae. *J Appl Physiol.* **2021**, 130, 342-354. Doi:10.1152/japplphysiol.00635.2020.
30. Kenville, R.; Maudrich, T., Vidaurre, C., Maudrich, D., Villringer, A., Ragert, P. et al. Intermuscular coherence between homologous muscles during dynamic and static movement periods of bipedal squatting. *J Neurophsiol.* **2020**, 124, 1045-1055. Doi:10.1152/jn.00231.2020.
31. Tanabe, H.; Fujii, K, Kouzaki, M. Joint coordination and muscle activities of ballet dancers during tiptoe standing. *Motor Control* **2017**, 21, 72-89. Doi:10.1123/mc.2015-0002.
32. Formaggio, E.; Masiero, S. Volpe, D., Demertzis, E., Gallo, L., Del Felice, A. Lack of inter-muscular coherence as axial muscles in Pisa Syndrome. *Neurol Sci.* **2019**, 40, 1465-1468. 10.1007/s10072-019-03821-7.
33. Mochizuki, G.; Semmler, J.G., Ivanova, T.D., Garland, S.J. Low-frequency common modulation of soleus motor unit discharge is enhanced during postural control in humans. *Exp Brain Res.* **2006**, 175(4), 584-595. https://doi.org/10.1007/s00221-006-0575-7.
34. Mochizuki, G.; Ivanova, T.D., Garland, S.J. Factors affecting the common modulation of bilateral motor unit discharge in human soleus muscles. *J Neurophysiol.* **2007**, 97, 3917-3925. doi:10.1152/jn.01025.2006.
35. Noé, F.; García-Massó, X., Paillard, T. Inter-joint coordination of posture on a seesaw device. *J Electromyogr Kinesiol.* **2017**, 34, 72-79. Doi:10.1016.j.elekin.2017.04.003.
36. Nandi, T.; Hortobagyi, T., van Keeken, H.G., Salem, G.J., Lamoth, C.J.C. Standing task difficulty related increase in agonist-agonist and agonist-antagonist common inputs are driven by corticospinal and subcortical inputs respectively. *Sci Rep.* **2019**, 9(1), 2439. doi: 10.1038/s41598-019-39197-z.
37. Ojha, A.; Alderink, G. Rhodes, S. Coherence between electromyographic (EMG) signals of anterior tibialis, soleus, and gastrocnemius during standing balance tasks. *Front Hum Neurosci.* **2023**, 17-2023, https://doi.org/10.3389/fnhum.2023.1042758.
38. Tsiouri, C.; Amiridis, I.G., Kannas, T., Varvariotis, N., Sahinis, C., Hazitaki, V., Enoka, R.M. EMG coherence of foot and ankle muscles increases with a postural challenge in men. *Gait Posture* **2024**, 113, 238-245. https://doi.org/10.1016/j.gaitpost.2024.06.019.
39. Alderink, G., McCrumb, D., Zeitler, D., Rhodes, S. Analysis of connectivity in electromyography signals to examine neural correlations in the activation of lower leg muscles for postural stability: A pilot study. *Bioengineering* 2025, 12, 84. https://doi.org/10.3390/bioengineering12010084.
40. Saffer, M.; Kiemel, T., Jeka, J. Coherence analysis of muscle activity during quiet stance. *Exp Brain Res.* **2008**, 185(2),215-226. https://doi.org/10.1007/s00221-007-1145-3.
41. Danna-Dos-Santos, A.; Boonstra, T.W., Degani, A.M., Cardoso, V.S., Magalhaes, T., Mochizuki, L., Leonard, C.T. Multi-muscle control during bipedal stance: an EMG-EMG analysis approach. *Exp Brain Res.* **2014**, 232(1), 75-87. doi: 10.1007/s00221-013-3721-z.
42. Kraskov, A., Stögbauer, H., Grassberger, P. Estimating mutual information. *Phys Rev E*. **2004**, 69, 066138. https://doi.org/10.1103/PhysRevE.69.066138.
43. Farmer. S.F.; Halliday, D.M., Conway, B.A., Stephens, J.A., Rosenburg, J.R. A review of recent applications of cross-correlation methodologies to human motor unit recording. *J Neurosi Methods* **1997**, 74, 175-187.
44. Pereda, E., Quiroga, R.Q., Bhattacharya, J. Nonlinear multivariate analysis of neurophysiological signals. *Prog Neurobiol*. **2005**, 77, 1-37. https://doi.org/10.1016/j.pneurobio.2005.10.003.
45. Jin, S.-H., Lin, P., Hallet, M. Linear and nonlinear information flow based on time-delayed mutual information method and its application to corticomuscular interaction. *Clin Neurophysiol*. **2010**, 121, 392-401. https://doi.org/10.1016/j.clinph.2009.09.033.
46. Shannon, C.E., The mathematical theory of communication. *Bell Syst Tech J*. **1948**, 27, 379-423, 623-656.
47. Cover, T.M., Thomas, J.A. *Elements of Information Theory*, 2nd ed.; John Wiley & Sons Inc.: Hoboken, New Jersey, USA, 2006.
48. Stone, J.V. *Information Theory, A Tutorial Introduction*, 1st ed.; Sebtel Press, 2015.
49. Delgado-Bonal, A., Marshak, A. Approximate entropy and sample entropy: A comprehensive tutorial. *Entropy* 2019, 21, 541. https://doi.org/10.3390/e21060541.

 doi:10.20944/preprints202604.0137.v1

50. Chen, C.-C., Hsieh, J.-C., Wu, Y.-Z., Lee, P.O., Chen, S.-S., Niddam, D.M., Yeh, T.-C., Wu, Y.-T. Mutual-information-based approach for neural connectivity during self-paced finger lifting task. *Hum Brain Mapp*. **2008**, 29,265-280.https://doi.org/10.1002/hbm.20386.
51. Jin, S.-H., Lin, P., Hallet, M. Linear and nonlinear information flow based on time-delayed mutual information method and its application to corticomuscular interaction. *Clin Neurophysiol*. **2010**, 121, 392-401. https://doi.org/10.1016/j.clinph.2009.09.033.
52. Sun, W., Liang, J., Yang, Y., Wu, Y., Yan, T., Song, R. Investigating age-related changes in the coordination of agonist and antagonist muscles using fuzzy entropy and mutual information. *Entropy* **2016**, 18, 229. https://doi.org/10.3390/e18060229.
53. Ó'Reilly, D., Delis, I. A network information theoretic framework to characterize muscle synergies in space and time. *J Neural Eng*. **2022**, 19, 016031. https://doi.org/10.1088/1741-2552/ac5150.
54. O'Reilly, D., Delis, I. Dissecting muscle synergies in the task space. *eLife* **2023**, 13, RP87651. https://doi.org/10.7554/eLife.87651.
55. O'Keeffe, R., Shirazi, S.,Y., Bilaloglu, S., Jahed, S., Bighamian, R., Raghavan, P., Atashzar, S.F. Nonlinear functional muscle network based on information theory tracks sensorimotor integration post stroke. *Sci Rep*. **2022**, 12, 130029. https://doi.org/10.1038/s41598-022-16483-x.
56. Kraskov, A. Synchronization and interdependence measures and their application to the electroencephalogram of epilepsy patients and clustering of data. Dissertation PhD thesis, University of Wuppertal, North Rhine-Westphalia, Germany, 2004. https://www.fz-juelich,de/nic-series/NIC-Series-e.html.
57. Cantú, H., Nantel, J., Millàn, M., Paquette, C., Cõte, J.N. Abnormal muscle activity and variability before, during, and after the occurrence of freezing in Parkinson's disease. *Fron Neurol*. **2019**, 10,951. https://doi.org/10.3389/fneur.2019.00951.
58. Ince, R.A.A., Giordano, B.L., Kayser, C., Rousselet, G.A., Gross, J., Schyns, P.G. A statistical framework for neuroimaging data analysis based on mutual information estimated via a Gaussian copula. *Hum Brain Mapp*. **2017**, 38, 1541-1573. https://doi.org/10.1002/hbm.23471.
59. Wang, Z., Hallac, R.R., Conroy, K.C., White, S.P., Kane, A.A., Collinsworth, A.L., Sweeney, J.A., Mosconi, M.W. Postural orientation and equilibrium processes associated with increased postural sway in autism spectrum disorder (ASD). *J Neurodev Dis*. **2016**, 8, 43. https://doi.org?10.1186/s11689-016-9178-1.
60. Bojanek, E.K., Wang, Z., White, S.P., Mosconi, M.W. Postural control processes during standing and step initiation in autism spectrum disorder. *J Neurodev Dis*. **2020**, 12,1. https://doi.org/10.1186/s11689-019-9305-x.
61. Boonstra, T.W., Faes, L., Kerkman, J.N., Marinazzo, D. Information decomposition of multichannel EMG to map interactions in the distributed motor system. *NeuroImage* **2019**, 202, 116093. https://doi.org/10.1016/j.neuroimage.2019.116093.
62. Faes, L, Porta, A., Nollo, G., Javorka, M. Information decomposition in multivariate systems: definitions, implementation and application to cardiovascular networks. *Entropy* 2017, 19,5. https://doi.org/10.3390/e19010005.
63. O'Reilly, D., Shaw, W., Hilt, P., de Castro Aguiar, R., Astill, S.L., Delis, I. Quantifying the diverse contributions of hierarchical muscle interactions to motor function. *IScience* **2025**, 28, 111613, https://doi.org/10.1016/j.isci.2024.111613.
64. Perotto, A.O. Anatomical guide for the electromyographer, 3rd ed.; Charles C. Thomas: Springfield, IL, USA, 2011; pp. 154-167.
65. Hermens, H.J.; Freriks, B., Disselhorst-Klug, C., Rau, G. Development of recommendations for SEMG sensors and sensor placement procedures. *J Electromyogr Kinesiol.* **2000**, 10(5), 361-74. Doi:10.1016/s1050-6411(00)00027-4.
66. Villaverde, A.F., Ross, J. Morán, F., Banga, J.R. MIDER: network inference with mutual information distance and entropy reduction. *PLos ONE* **2014**, 9(5), e96732. https://doi.org/10.1371/journal.pone.0096732.
67. Cellucci, C.J., Albano, A.M., Rapp, P.E. Statistical validation of mutual information calculations: comparison of alternative numerical algorithms. *Phys Rev E*. **2005**, 71, 66208. https://doi.org/10.1103/PhysRevE.71.066208.

 doi:10.20944/preprints202604.0137.v1

68. R Core Team (**2024**), R: A language and environment for statistical computing. R Foundation for Statistical Computing. Vienna, Austria. Htttps://www.R-project.org. (accessed 10 June 2024).
69. Posit Team (**2024**), RStudio: Integrated Development Environment for R.Posit Software, PBC, Boston, MA. https://www.posit.co/. (accessed 10 June 2024).
70. Latash, M.L.; Scholz, J.P., Schöner, G. Motor control strategies revealed in the structure of motor variability. *Exerc Sport Sci Rev.* **2002**, 30(1), 26-31. doi: 10.1097/00003677-200201000-00006.
71. Latash, M.L. The bliss (not the problem) of motor abundance (not redundancy). *Exp Brain Res.* **2012**, 217, 1-5. Doi:10.1007/s002221-012-3000-4.
72. Latash, M.L. Motor synergies and the equilibrium-point hypothesis. *Mot Contr.* **2020**, 14, 294-2010. Doi:10.1123/mcj.14.3.294.
73. Proferta, V.L.,Turvey, M.T. Berstein's levels of movement construction: A contemporary perspective. *Hum Mov Sci*. **2018**, 57, 111-133. https://doi.org/10.1016/j.humov.2017.11.013.
74. Scholz, J.P., Schöner, G. The uncontrolled manifold concept: Identifying control variables for a functional task. *Exp Brain Res*. **1999**, 126, 289-306. https://doi.org/10.1007/s002210050738.
75. Boonstra, T.W., Breakspear, M. Neural mechanisms of intermuscular coherence: Implications for the rectification of surface electromyography. *J Neurophysiol*. **2011**, 107, 796-807. https://doi.org/10.1152/jn.00066.2011.
76. Semmler, J.G. Motor unit synchronization and neuromuscular performance. *Exer Sport Sci Rev*. **2002**, 30, 8-14. https://doi.org/10.1097/00003677-200201000-00003.
77. Danna-Dos-Santos, A.; Degani, A.M., Boonstra, T.W., Mochizuki, L., Harney, A.M., Schmeckpeper, M.M., Tabor, L.C., Leonard, C.T. The influence of visual information on multi-muscle control during quiet stance: a spectral analysis approach. *Exp Brain Res.* **2015**, 233(2), 657-669. 10.1007/s00221-014-4145-0.
78. De Luca, C.J.; Erim, Z. Common drive in motor units of a synergistic muscle pair. *J Neurophysiol.* **2002**, 87(4), 2200-2204. https://doi.org/10.1152/jn.00793.2001.
79. Farmer, S.G. Rhythmicity, synchronization and binding in human and primate motor systems. *J Physiol.* **1998**, 509(Pt 1), 3-14.
80. Bizzi, E.; Cheung, V.C.K. The neural origin of muscle synergies. *Front Comput Neurosci.* **2013**, 7 - 2013. Doi:10.3389/fncom.2013.00051.
81. Laine, C.M.; Valero-Cuevas, F.J. Intermuscular coherence reflects functional coordination. *J Neurophysiol* **2017**, 118, 1775-1783.
82. Kerkman, J.N.; Daffertshofer, A., Gollo, L.L., Breakshpear, M., Boonstra, T.W., Network structure of the human musculoskeletal system shapes neural interactions on multiple time scales. *Sci Adv.* **2018**, 4(6), eaat0497. doi: 10.1126/sciadv.aat0497.
83. Boonstra, T.W.; Roerdink. M., Daffertshofer, A., van Vugt, B., van Werven, G., Beek, P.J. Low-alcohol doses reduce common 10- to 15-Hz input to bilateral leg muscles during quiet standing. *J Neurophysiol.* **2008**, 100(4),2158-2164. https://doi.org/10.1152/jn.90474.2008.
84. Obata, H.; Abe, M.O., Masani, K., Nakazawa, K. Modulation between bilateral legs and within unilateral muscle synergists of postural muscle activity changes with development and aging. *Exp Brain Res.* **2014**, 232(1), 1-11. doi: 10.1007/s00221-013-3702-2.
85. Degani, A.M., Leonard, C.T., Danna-Dos-Santos, A. The use of intermuscular coherence analysis as a novel approach to detect age-related changes in postural synergy. *Neurosci Lett*. **2017**, 656, 108-113. https://doi.org/10.1016/j.neulet.2017.07.032.
86. Degani, A.M., Leonard, C.T., Danna-Dos-Santos, A. The effects of aging on the distribution and strength of correlated neural inputs to postural muscles during unperturbed bipedal stance. *Exp Brain Res*. **2020**, 238, 1537-1553. https://doi.org/10.1007/s00221-020-05837-4.
87. Watanabe, T., Saito, K., Ishida, K., Tanabe, S., Nojima, I. Age-related changes in the ability to modulate common input to bilateral and unilateral plantar flexors during forward postural lean. *Front Hum Neurosci*. **2018**, 12, 254. https://doi.org/10.3389/fnhum.2018.00254.
88. Walker, S., Piitulainen, H., Manlangit, T., Avela, J., Baker, S.N. Older adults show elevated intermuscular coherence in eyes-open standing by only young adults increase coherence in response to closing the eyes. *Exp Physiol*. **2020**, 105, 1000-1011. https://doi.org/10.1113/EP088468.

 doi:10.20944/preprints202604.0137.v1

89. Yamanake, E.; Horiuchi, Y., Nojima, I. EMG-EMG coherence during voluntary control of human standing tasks: a systematic scoping review. *Front Neurosci.* **2023**, 17, 1145751. Doi:10.3389/fnins.2023.1145751.
90. García-Massó, X.; Pellicer-Chenoll, M. Gonzalez, L.M., Toca-Herrera, J.L. The difficulty of the postural control task affects multi-muscle control during quiet standing. *Exp Brain Res.* **2016**, 234(7), 1977-1986. doi: 10.1007/s00221-016-4602-z.
91. Watanabe, T.; Saito, K., Ishida, K., Tanabe, S., Nojima, I. Fatigue-induced decline in low-frequency common input to bilateral and unilateral plantar flexors during quiet standing. *Neurosci Lett.* **2018c**, 686, 193-197. Doi:10.1016/j.neulet.2018.09.019.
92. Glass, S.M.; Wildman, L., Brummitt, C., Ratchford, K., Westbrook, G.M., Aron, A. Effects of global postural alignment on posture-stabilizing synergy and intermuscular coherence in bipedal standing. *Exp Brain Res.* **2022**, 240, 841-851. https://doi.org/10.1007/s00221--021-06291-6.
93. Nandi, T., Fisher, B.E., Hortobágyi, T., Salem, G.J. Increasing mediolateral standing sway is associated with increasing corticospinal excitability, and decreasing M1 inhibition and facilitation. Gait Posture 2018, 60, 135-140. https://doi.org/10.1016/j.gaitpost.2017.11.021.
94. Torres-Oviedo, G., Ting, L.H. Subject-specific muscle synergies in human balance control are consistent across different biomechanical contexts. *J Neurophysiol*. **2010**, 13, 9259. https://doi.org//10.1152/jn.00960.2009.
95. Montesinos, L., Castaldo, R., Pecchia, L. On the use of approximate entropy and sample entropy with centre of pressure time series. *J Neuroeng Rehabil*. **2018**, 15, 116. https://doi.org/10.1186.s12984-018-0465-9.
96. Pincus, S.M., Gladstone, I.M., Ehrenkranz, R.A. A regularity statistic for medical data analysis. *J Clin Monit*. **1991**, 7(4), 335-45. https://doi.org/10.1007/BF01619355.
97. Richman, J.S., Moorman, J.R. Physiological time-series analysis using approximate entropy and sample entropy. *Am J Physiol Heart Circ Physiol*. **2000**, 278(6), H2039-49. https://doi.org/10.1152/ajpheart.2000.278.6.H2039.
98. Tipton, N., Alderink, G., Rhodes, S. Approximate entropy and the velocity of center of pressure to determine postural stability: A pilot study. *Appl Sci*. **2023**, 13, 9259. https://doi.org/10.3390/appl13169259.
99. Wesley, J., Rhodes, S., Zeitler, D.W., Alderink, G. Approximate and sample entropy of the center of pressure during unperturbed tandem standing: Effect of altering the tolerance window. *Appl Sci*. **2025**, 15(2), 576. https://doi.org/10.3390/appl15020576.
100. Morasso, P.; Cherif, A., Zenzeri, J. Quiet standing: the single inverted pendulum model is not so bad after all. *PLoS One* **2019**, 14(3), e0213870. doi: 10.1371/journal.pone.0213870.
101. Gunther, M.; Grimmer, S., Siebert, T., Blickhan, R. All joints contribute to quiet stance: a mechanical analysis. *J Biomech.* **2009**, 42, 2739-2746. DOI: 10.1016/j.biomech.2009.08.014.
102. Suzuki, Y.; Nomura, T., Casadio, M., Morasso, P. Intermittent control with ankle, hip, and mixed strategies during quiet standing: a theoretical proposal based on a double inverted pendulum model. *J Theor Biol.* **2012**, 310, 55-79. http://dx.doi.org/10.1016/j.jtbi.2012.019.
103. Sasagawa, S.; Shinya, M., Nakazawa, K. Interjoint dynamic interaction during constrained human quiet standing by induced acceleration analysis. *J Neurophysiol.* **2014**, 111, 313-322. DOI: 10.1152/jn.01082.2012.